



Paleoceanography and Paleoclimatology[®]

RESEARCH ARTICLE

10.1029/2023PA004730

Key Points:

- · The modified sample loading technique adopted for X-ray diffraction significantly reduced the uncertainty of calcite measurement down to 0.33%
- Temperature reconstructions based on Sr/Ca, Li/Mg, and Li/Ca are significantly affected by low levels of intra-skeletal calcite (1%-2%)
- Impact of low levels of intra-skeletal calcite on δ¹⁸O, Ba/Ca, Mn/Ca, and U/ Ca is not significant

Supporting Information:

Supporting Information may be found in the online version of this article.

Correspondence to:

M. M. Weerabaddana. mudithw@arizona.edu

Citation:

Weerabaddana, M. M., Thompson, D. M., Reed, E. V., Farfan, G. A., Kirk, J. D., Kojima, A. C., et al. (2024). Impact of intra-skeletal calcite on the preservation of coral geochemistry and implications for paleoclimate reconstruction. Paleoceanography and Paleoclimatology,

39, e2023PA004730. https://doi.org/10. 1029/2023PA004730

Received 5 AUG 2023 Accepted 12 APR 2024

Author Contributions:

Conceptualization: Mudith M. Weerabaddana, Diane M. Thompson, Emma V. Reed

Data curation: Mudith M. Weerabaddana. Diane M. Thompson, Emma V. Reed, Gabriela A. Farfan, David L. Dettman Formal analysis: Mudith

M. Weerabaddana

Funding acquisition: Diane

M. Thompson

Investigation: Mudith M. Weerabaddana, Diane M. Thompson

Methodology: Mudith M. Weerabaddana, Diane M. Thompson, Emma V. Reed, Gabriela A. Farfan, Jason D. Kirk Project administration: Diane M. Thompson, Kalena de Brum, Emma Kabua, Florence Edwards Resources: Diane M. Thompson, Emma V. Reed, Gabriela A. Farfan, Jason D. Kirk, David L. Dettman,

© 2024. American Geophysical Union. All Rights Reserved.

Impact of Intra-Skeletal Calcite on the Preservation of Coral **Geochemistry and Implications for Paleoclimate** Reconstruction

Mudith M. Weerabaddana¹, D. Diane M. Thompson¹, Emma V. Reed¹, Gabriela A. Farfan², Jason D. Kirk¹, Alice C. Kojima¹, David L. Dettman¹, Kalena de Brum³, Emma Kabua⁴, and Florence Edwards⁴

¹Department of Geosciences, University of Arizona, Tucson, AZ, USA, ²Department of Mineral Sciences, Smithsonian National Museum of Natural History, Washington, DC, USA, 3School of Aquatic and Fisheries Sciences, University of Washington, Washington, DC, USA, 4Marshall Islands Marine Resources Authority, Delap-Uliga-Djarrit, Marshall Islands

Abstract The geochemistry of tropical coral skeletons is widely used in paleoclimate reconstructions. However, sub-aerially exposed corals may be affected by diagenesis, altering the aragonite skeleton through partial dissolution, or infilling of secondary minerals like calcite. We analyzed the impact of intra-skeletal calcite on the geochemistry (δ¹⁸O, Sr/Ca, Mg/Ca, Li/Mg, Li/Ca, U/Ca, B/Ca, Ba/Ca, and Mn/Ca) of a subaerially exposed Porites sp. coral. Each micro-milled coral sample was split into two aliquots for geochemistry and X-ray diffraction (XRD) analysis to quantify the direct impact of calcite on geochemistry. We modified the sample loading technique for XRD to detect low calcite levels (1%–2%; total uncertainty = 0.33%, 2σ) in small samples (~7.5 mg). Calcite content ranged from 0% to 12.5%, with higher percentages coinciding with larger geochemical offsets. Sr/Ca, Li/Mg, Li/Ca, and δ¹⁸O-derived sea-surface temperature (SST) anomalies per 1% calcite were +0.43°C, +0.24°C, +0.11°C, and +0.008°C, respectively. A 3.6% calcite produces a Sr/Ca-SST signal commensurate with local SST seasonality (~1.5°C), which we propose as the cut-off level for screening calcite diagenesis in paleo-temperature reconstructions. Inclusion of intra-skeletal calcite decreases B/Ca, Ba/ Ca, and U/Ca values, and increases Mg/Ca values, and can therefore impact reconstructions of paleoclimate and the carbonate chemistry of the semi-isolated calcifying fluid in corals. This study emphasizes the importance of quantifying fine-scale calcite diagenesis to identify coral preservation levels and assure robust paleoclimate reconstructions.

1. Introduction

Modern scleractinian corals secrete aragonite (calcium carbonate) skeletons, the geochemistry of which are a function of the environment in which they grow. These skeletons incorporate an array of trace metals, radiogenic isotopes, and stable isotopes that serve as tracers for changes in the tropical marine environment and biomineralization (Corrège, 2006; Lough & Cooper, 2011; Thompson, 2021). Therefore, the skeletal geochemistry of long-lived corals can be used to reconstruct past marine environmental changes such as sea-surface temperature (SST), sea-surface salinity (SSS), pH, ocean production, upwelling, river runoff, wind stress, and ocean circulation (e.g., Douville et al., 2010; Grothe et al., 2020; Hathorne, Felis, et al., 2013; Kojima et al., 2022; McCulloch et al., 2003; Montaggioni et al., 2006; Reed et al., 2022; Thompson et al., 2015; Watanabe et al., 2021). However, the quality of reconstruction depends on the level of preservation of such geochemical signals that are subject to alteration due to external perturbation; when assessed properly, coral-based climate reconstructions may extend instrumental records by several thousands of years (e.g., Brocas et al., 2018; Cobb et al., 2013; Felis et al., 2015; Grothe et al., 2020; Tudhope et al., 2001).

Diagenesis alters the primary aragonite crystallography and its geochemistry in both submarine and sub-aerial environments (Hendy et al., 2007; Lazareth et al., 2016; Nothdurft & Webb, 2009; Sayani et al., 2011). Dissolution of the aragonite skeleton, precipitation of secondary aragonite or calcite, calcite cementation, and/or recrystallization with calcite replacement occurs during diagenesis (McGregor & Gagan, 2003; Sayani et al., 2011). The type of diagenesis and its extent depends on the environmental setting to which the coral is exposed. For example, skeletal dissolution is accelerated under a tropical humid climate. Further, as corals are porous and have a honeycomb-like skeletal architecture, sub-aerially exposed corals mimic the vadose zone, where unsaturated fresh water (meteoric water) in contact with air infiltrates the porous coral skeleton. As water



10.1029/2023PA004730

Kalena de Brum, Emma Kabua, Florence Edwards Software: Gabriela A. Farfan, Jason D. Kirk, Alice C. Kojima Supervision: Diane M. Thompson Validation: Mudith M. Weerabaddana, Diane M. Thompson, Emma V. Reed. Gabriela A. Farfan, Alice C. Kojima Visualization: Mudith M. Weerabaddana Writing - original draft: Mudith M. Weerabaddana Writing - review & editing: Mudith M. Weerabaddana, Diane M. Thompson, Emma V. Reed, Gabriela A. Farfan, Jason D. Kirk, Alice C. Kojima, David L. Dettman, Kalena de Brum,

Emma Kabua, Florence Edwards

percolates slowly through the coral skeleton, the dissolution and precipitation zones are separated by a thin film of water over the inner surfaces of the coral (Longman, 1980; Pingitore, 1976). Enhanced evaporation further saturates the solution phase and thus facilitates the precipitation of secondary materials such as calcite onto subaerial coral skeletons (Longman, 1980). Different levels of dissolution can change from pristine aragonite to chalky, melted-like, or etched surfaces and eventually to complete cementation, where a thin layer of calcite is deposited on top of the aragonite skeletal surface after dissolution (Hendy et al., 2007; McGregor & Gagan, 2003). Blocks of calcite crystals may also grow at discrete regions inside the porous skeleton forming intra-skeletal calcite. Nonetheless, calcite cementation is the most common diagenetic alteration of subaerially exposed corals (James, 1974b) and the most well-studied to date.

Submarine diagenesis is less common but has been reported in several studies (Allison et al., 2007; Lazareth et al., 2016; Quinn & Taylor, 2006; Sayani et al., 2011). Lazareth et al. (2016) reports early submarine calcite diagenesis in live collected corals of up to 32% due to the freshening of seawater that facilitates dissolution and calcite precipitation. The high strontium (Sr) contents in seawater make coral aragonite skeletons thermodynamically unstable and prone to dissolution (Finch & Allison, 2003). Dissolution promotes calcite formation and may therefore impart non-climate artifacts on stable isotope and trace elemental signatures. Additionally, bioerosion by micro or macro-burrowers (mostly macro-crustaceans like bivalves that burrow into the coral) creates microenvironments within live corals and provides pathways for seawater to infiltrate the coral skeletons (see Figures 1g-1i). Such secondary interactions can trigger dissolution and secondary aragonite cementation, especially in the upper layers of the coral.

As with secondary calcite diagenesis, secondary aragonite formation results in a non-climate-related offset in skeletal geochemistry (Nothdurft et al., 2007; Nothdurft & Webb, 2009). Secondary aragonite is composed of blunt aragonite needles, in contrast to the sharp and long aragonite needles in acicular bundles that make up the coral skeleton. Inorganic precipitation of secondary aragonite can be detected in submarine diagenesis that is characterized by high Sr/Ca and δ^{18} O values compared to biogenically-precipitated aragonite (Hendy et al., 2007; Müller et al., 2001; Sayani et al., 2011), producing a cool temperature offset of up to \sim 1–2°C (Allison et al., 2007; Hendy et al., 2007). Finally, dissolution in submarine environments is also known to produce temperature anomalies colder than ambient SST (Allison et al., 2007), but the extent of the effect of dissolution on individual geochemical proxies is not well studied. Levels of dissolution are difficult to quantify and are typically only observed visually using SEM.

Previous work has demonstrated the large impacts of calcite diagenesis on the geochemical proxies used to reconstruct past climate variability. For example, values of temperature-sensitive proxies such as δ^{18} O, Sr/Ca, Li/Ca, and Li/Mg have been shown to decrease with increasing levels of calcite diagenesis. Such calcite inclusions create warm temperature offsets (up to $\sim 2-4^{\circ}$ C depending on the level of diagenesis) that are not explained by climate alone (Griffiths et al., 2013; McGregor & Gagan, 2003; Nothdurft et al., 2007; Sayani et al., 2011). Considering the high rainfall and humid tropical climate, many sub-fossil corals used in previous studies may have had calcite diagenesis to various extents. Diagenesis in sub-aerially exposed corals is likely to contain both calcite cement and intra-skeletal calcite (Griffiths et al., 2013; McGregor & Gagan, 2003; Rabier et al., 2008) which needs to be visually differentiated using scanning electron microscopy (SEM). Further, the level of the effect of diagenesis on temperature reconstruction can also vary according to the nature of the calcite (i.e., calcite cement vs. intra-skeletal calcite) (Lazareth et al., 2016).

In addition to the coral paleotemperature proxies, U/Ca, B/Ca, Mn/Ca, and Ba/Ca can be used to understand environmental conditions such as seawater pH (Inoue et al., 2011), coral biomineralization (Montagna et al., 2007; Sinclair, 2005), Pacific trade winds (Kojima et al., 2022; Thompson et al., 2015), upwelling, and river-runoff (Lewis et al., 2018). Only a few studies have assessed the effects of diagenetic calcite on these important geochemical proxies. Previous studies have shown that the presence of calcite cement in corals results in reduced B/Ca values and increased U/Ca (Allison et al., 2007). However, similar studies have also argued that both B/Ca and U/Ca decrease with increasing calcite diagenesis (Griffiths et al., 2013; Lazareth et al., 2016). Additionally, the effect of calcite on coral Mn/Ca has not been studied. Coral Mn/Ca is a proxy for trade winds in the tropical Pacific (originally studied by Shen et al. (1992) and later expanded by Thompson et al. (2015) and Sayani et al. (2021)) and is important in reconstructing changes associated with the El Niño-Southern Oscillation (ENSO). Therefore, prescreening corals for calcite diagenesis and evaluating its effect on geochemistry is important to assure a quality paleoclimate reconstruction.

WEERABADDANA ET AL. 2 of 19

1.1. Coral Screening for Diagenesis

Screening for diagenesis when using fossil corals in paleoclimate reconstructions is a common practice. Typically, a few discrete samples from the top, middle, and bottom of the coral core are examined for diagenesis using XRD, SEM, and thin-sections; the top and the bottom of the coral being the most susceptible to alteration (Thompson, 2021). The extent of effort put into screening for diagenesis in early studies is remarkable (Bar-Matthews et al., 1993; Gvirtzman et al., 1973; James, 1974b; Macintyre & Towe, 1976; McGregor & Gagan, 2003; Nothdurft & Webb, 2008). Diagenetic alterations are often visible in X-radiograph images as dark areas relative to the rest of the core permitting these regions to be readily excluded from sampling (Felis et al., 2012). However, there can be fine-scale, intra-skeletal diagenesis anywhere in the coral depending on the time and frequency of exposure to external perturbations such as rainfall that may not be detected either via X-radiography or discrete sampling for XRD and SEM.

The crystallographic replacement or overgrowth of orthorhombic aragonite needles by trigonal calcite rhombs can be visually observed using SEM and/or thin-section analysis (Allison et al., 2007; Griffiths et al., 2013; Hendy et al., 2007; Lazareth et al., 2016; McGregor & Abram, 2008). Petrographic thin-sections of coral skeletons are usually stained to enhance calcite and aragonite textural characteristics due to their similar optical properties under plain-polarized and cross-polarized light (McGregor & Abram, 2008). Similarly, films of carbon, gold, or platinum increase the conduction of charge of the electron beam and enhance fine details of the surface of the coral under SEM. Qualitative analysis of high-resolution SEM images and coral thin-sections are used to visually assess fine-scale details of crystal structure, skeletal architecture, and diagenetic alterations (McGregor & Abram, 2008). SEM images and coral thin-sections also provide visual evidence of the type and origin of diagenesis by microstructural (needle-like aragonite vs. calcite blocks) and textural (chalky vs. cement) differences (Allison et al., 2007; Griffiths et al., 2013; Lazareth et al., 2016; Rabier et al., 2008). However, diagenetic alterations cannot be quantified via SEM or thin-section imaging.

X-ray powder diffraction (XRD) is used in the quantification and phase identification of minerals present in powdered coral samples (Rahman et al., 2013). XRD can detect the relative presence of aragonite and calcite in coral samples, which is converted into weight or molar percentages after calibration (Vyverberg et al., 2018). Although XRD can differentiate primary aragonite from calcite, it cannot isolate (and thus, quantify) secondary aragonite which can also alter the primary geochemistry of coral carbonate (Allison et al., 2007; Enmar et al., 2000; Hendy et al., 2007). Thus, combining XRD with SEM and thin-section screening is an effective way to determine coral skeletal preservation.

Mainstream XRD methods require large sample masses and have poor reproducibility, limiting their ability to detect calcite in individual samples whose geochemistry will also be analyzed. Nonetheless, early studies used a discreet and bulk sampling approach permitting researchers to identify and exclude areas of calcite diagenesis (Felis et al., 2014; Lazareth et al., 2016; Quinn & Taylor, 2006; Rashid et al., 2020). Current powder sample analysis methods require large amounts of coral powder for XRD analysis (e.g., 2-3 g in Dechnik et al. (2017) and 100-200 mg in McGregor and Abram (2008)), precluding a direct comparison of the effect of diagenesis on the geochemistry of the same sample. More recently, Smodej et al. (2015) proposed a fast, non-destructive screening method (SD error <1%) that can detect calcite in corals at a high spatial resolution, permitting diagenetic sections to be excluded from geochemical sampling. Still, conventional calcite quantification methods using XRD are not accurate below 1% calcite due to the high error associated with the measurement. Their reproducibility at low calcite levels (1%-2%) is poor due to inconsistencies in sample loading and XRD analysis techniques (Dutton et al., 2015; McGregor & Abram, 2008; Vyverberg et al., 2018). These limitations are critical, as 1%-2% calcite in corals used in paleoclimate reconstructions may modify original climate signals and may lead to erroneous paleoclimate interpretations. Due to the sampling size requirements, studies to date that investigate calcite diagenesis have used bulk sample materials from the coral at discrete intervals that do not represent a direct effect on the geochemistry of the same sample used in paleoclimate studies.

In this study, we adopt simple techniques to improve the reproducibility and accuracy of traditional coral powder XRD analysis. By using the modified XRD method we assess the impact of intra-skeletal calcite diagenesis on the geochemistry of the same micro sample collected at a millimeter scale. As opposed to traditional discrete sampling, our approach detects isolated spots where intra-skeletal calcite is present above a threshold along a continuous sampling path and therefore allows us to eliminate altered individual samples from the final reconstruction. Further, we evaluate the effect of intra-skeletal trace-calcite on an extensive array of coral geochemical

WEERABADDANA ET AL. 3 of 19

25724525, 2024, 5, Downloaded from https://agupubs.onlinelibrary.wiley.com/doi/10.1029/2023PA004730 by University Of Arizona Library, Wiley Online Library on [03/05/2024]. See the Terms and Conditions (https://agupubs.onlinelibrary.wiley.com/doi/10.1029/2023PA004730 by University Of Arizona Library, Wiley Online Library on [03/05/2024]. See the Terms and Conditions (https://agupubs.onlinelibrary.wiley.com/doi/10.1029/2023PA004730 by University Of Arizona Library, Wiley Online Library on [03/05/2024]. See the Terms and Conditions (https://agupubs.onlinelibrary.wiley.com/doi/10.1029/2023PA004730 by University Of Arizona Library.

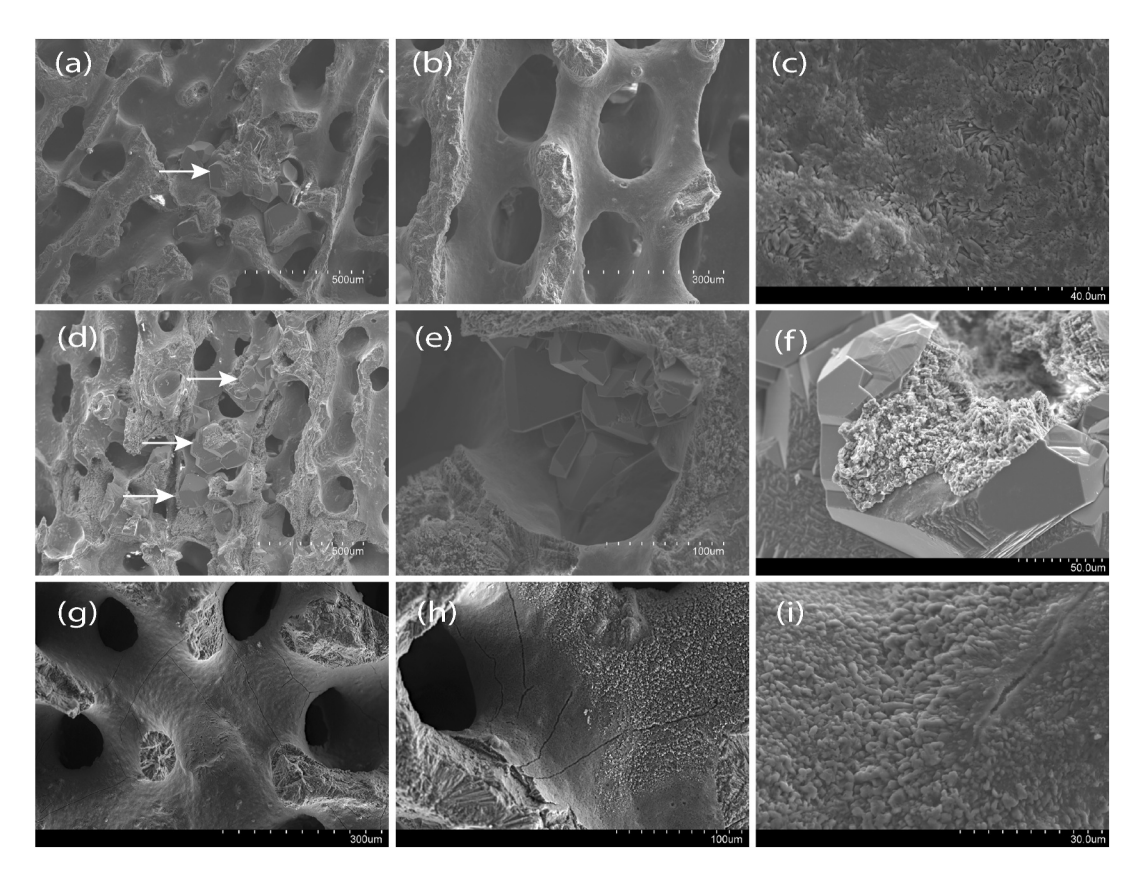


Figure 1. Secondary electron scanning electron photomicrographs of the coral skeleton. (a–c) Pristine aragonite skeleton from core depths of 15–30 mm (above the section of diagenesis). (d–f) Intra-skeletal calcite within the diagenetically altered section from core depths of 56–155 mm. Calcite overgrowths are shown in white arrows. (e) Calcite within a pore space. (f) High-resolution image of a single calcite crystal. (g–i) Partially altered skeleton due to dissolution from core depths of 795–800 mm. Note the micro-boring tracks in h and i leading to dissolution surfaces. Calcite percentages measured in XRD in a-c sections are <2% and, (e)–(f) sections are 4%–12%. Calcite is not visible in (g)–(i) sections of the coral.

proxies (four temperature-sensitive proxies and five other proxies, including novel Mn/Ca trade-wind proxy) and their implications for paleoclimate interpretations.

2. Methods

2.1. Coral Sampling and Preparation

A \sim 1.2 m cylindrical core (in six sections) was collected from a subfossil (remains of organisms that are neither true fossils nor modern; hereafter referred to as "fossil") *Porites* sp. coral boulder in January 2018 from Majuro Atoll, Marshall Islands (7.1°N, 171.4°E) (Figures S1a in Supporting Information S1). The coral boulder had previously been transported inland, painted, and placed in a parking lot, where it had been sitting for an unknown number of years (Figure S1b in Supporting Information S1). The team used a gas-powered drill with a 2.5-inch diameter diamond-tipped drill bit to vertically drill from the top center of the coral along the primary growth axis to obtain a core sample (hereafter MAJ18-2). Cores were cut into \sim 5 mm thick slabs using a custom-built computerized saw at the Australian Institute of Marine Science. The middle slice of each core section is used for subsequent analyses to maintain consistency throughout the core. The slabs were water-picked and ultrasonicated using Milli-Q water to remove non-matrix bound organic matter, dust, and coral cuttings, and subsequently dried.

Digital X-radiographs of the coral slabs were taken using an EcoRay Orange 1040HF X-radiograph machine (Figure S2 in Supporting Information S1). These X-radiographs were examined to identify optimum sampling paths along the maximum growth axis in areas with optimal skeletal architecture (DeLong et al., 2013; Reed et al., 2021). Corals were initially screened for diagenesis by visual assessment of X-ray images. The distance between light and dark growth band couplets in the X-radiographs was measured for each year (Knutson

WEERABADDANA ET AL. 4 of 19



10.1029/2023PA004730

et al., 1972) to determine the micro-sampling interval necessary to achieve at least monthly sampling resolution. Based on an average extension rate of \sim 15 mm/year, samples were milled at continuous 1.0 mm increments, resulting in better than monthly sampling resolution.

2.2. Geochemical Analysis

An automated tri-axial micro mill system (NexGen-model 5810 from Sherline Products, Inc. California) was used to extract continuous micro-samples from the coral slab surface along the maximum growth axis perpendicular to growth bands. Each sample (~10-15 mg) was collected using a 3.2 mm diameter drill bit in 1.0 mm increments along 3.0 mm deep and 6.0 mm wide transects. Coral powder samples were weighed (0.55-0.65 mg) on a microbalance (±0.01 mg) and digested in ultra-pure (doubly distilled) 2% HNO₃ acid. We used an Element 2 inductive coupled plasma mass spectrometer at the Tropical Climate and Coral Reefs Laboratory at the University of Arizona to analyze trace elemental concentrations (Sr, Ca, Mg, Li, Mn, B, Ba, and U) in 863 micro-samples. We used indium (In¹¹⁵) at a concentration of 2 mg/L as an internal standard mixed into every sample by the ESI FAST autosampler to check and correct for instrumental drift within each analytical run. Additionally, an external matrix-matched check standard (S2) made to resemble the trace element concentration in the coral skeleton using high-purity single-element standards was used to correct for instrumental drifts among runs (Schrag, 1999). An in-house coral standard (MCP) was used as an external reference for reproducibility, analyzed after approximately every six coral samples. Precisions for MCP are reported in Table S6 in Supporting Information S1. The international coral standard JCp-1 (Hathorne, Gagnon, et al., 2013; Okai et al., 2002) was measured twice in each analysis run as a second external reference standard (precisions are reported in Table S5 in Supporting Information S1). All external standards were treated the same way as the samples.

Aliquots of the same samples were used for stable isotope measurements. $\delta^{18}O$ values of carbonates were measured using an automated carbonate preparation device (KIEL-III) coupled to a gas-ratio mass spectrometer (Finnigan MAT 252). Powdered samples were reacted with dehydrated phosphoric acid under vacuum at 70°C. The isotope ratio measurement is calibrated based on repeated measurements of internal standard NBS-19 and the precision for $\delta^{18}O$ is $\pm 0.10\%$ (1σ , n=186). All the measured stable isotope values are reported per mill (%) relative to the Vienna Pee Dee Belemnite (VPDB) standard notation.

2.3. Age Model

A coral sample taken close to the bottom of the MAJ18-2 coral was age-dated using the U/Th dating technique using a Nu Plasma II-ES MC-ICP-MS at the Massachusetts Institute of Technology (Cheng et al., 2013; Cobb et al., 2003). The chronology of the MAJ18-2 coral was constructed by matching seasonal cycles in $\delta^{18}O$ with instrumental SST data from Majuro Island and annual density bands in the X-radiograph. The maximum and minimum $\delta^{18}O$ values were tied to minimum (winter) and maximum (summer) peaks of the seasonal SST cycle, respectively, to constrain the age-depth tie points. We used $\delta^{18}O$ monthly cycles as a better indicator of the seasonal cycle at the Republic of Marshall Islands (RMI) to build a robust age model because the hydrology of the tropical Pacific largely influences the coral $\delta^{18}O$ signature and amplifies the seasonal signal (Reed et al., 2022; Thompson et al., 2022). The MAJ18-2 chronology was cross-checked with U/Th dating done at the base of the MAJ18-3 coral core, a co-located colony whose growth overlaps in the same time interval. Time assignment for coral geochemistry and interpolation among tie-points were performed using the MATLAB code written by T. R. Ault (2007) from the age-depth model created from the tie-points and the raw geochemical data by depth. Age-modeled records were compared with monthly SST data from Extended Reconstructed Sea Surface Temperature (ERSST) v5 (Huang et al., 2017) from a $2^{\circ} \times 2^{\circ}$ grid box centered on Majuro Island (7.1°N, 171.4°E) to assess the quality of the age model. All coral geochemical proxies were interpolated to monthly resolution to compare with monthly climatology.

2.4. Detection and Quantification of Calcite Diagenesis

The top, bottom, and a few selected areas including every piece of the coral core were imaged using a Hitachi S-3400N scanning electron microscope (Figure S2 in Supporting Information S1). Coral fragments of $\sim 1-2$ cm² from selected areas of each core piece were cut using a Dremel cutting tool (see Figure S2 in Supporting Information S1 for details), cleaned with milli-Q water using a water pick, and sonicated for at least 10 min to remove cutting dust. The cut fragments were sputter-coated with an ultra-fine carbon coat and observed in SEM at

WEERABADDANA ET AL. 5 of 19

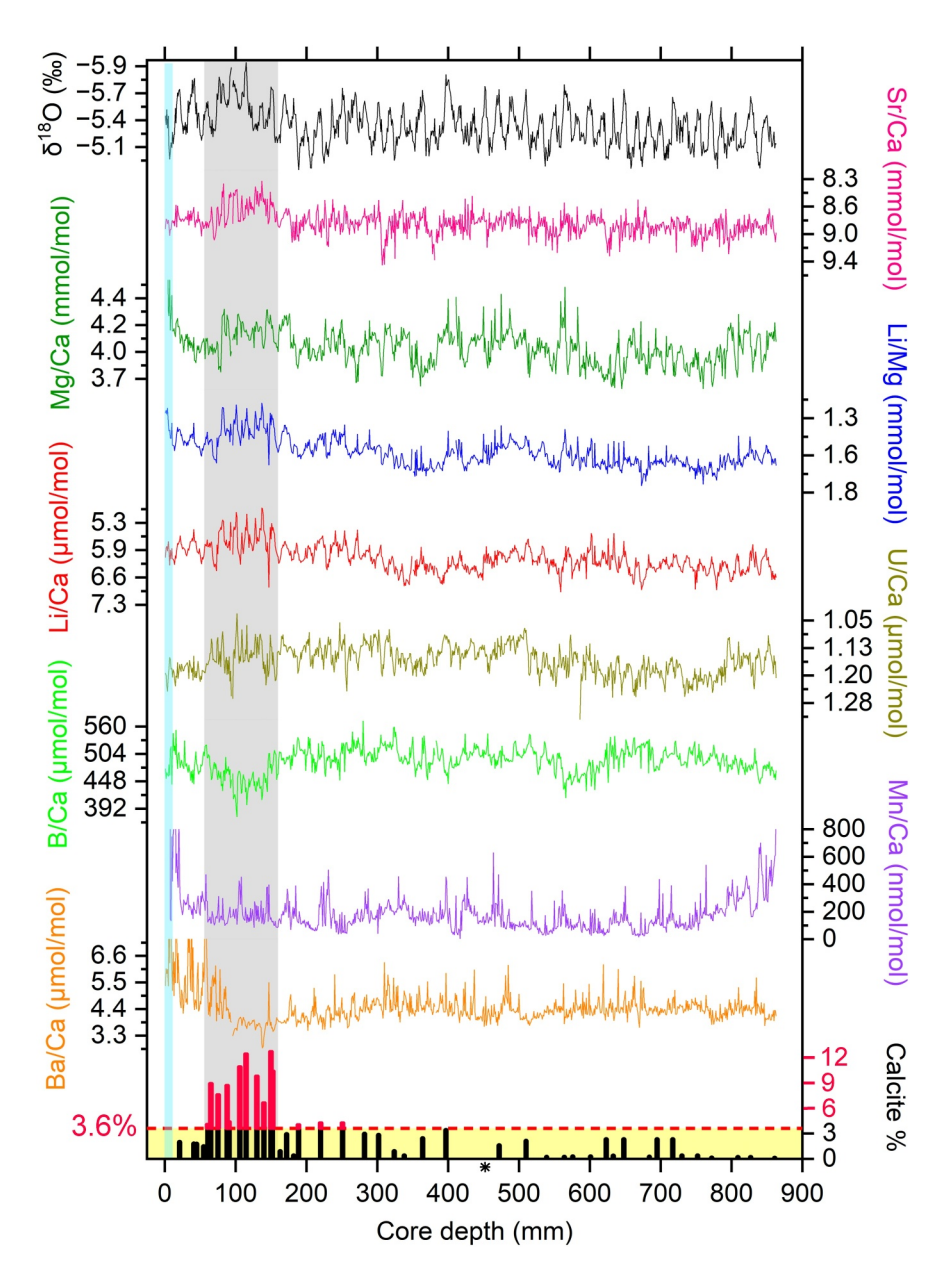


Figure 2. Transects across MAJ18-2 coral core (in mm increments) demonstrating shifts in geochemistry compared to calcite content. Bars at the bottom are the calcite percentages measured in individual samples. The diagenetically altered section with higher calcite percentages is highlighted in gray with extended red bars when the calcite percentage exceeds 3.6%. Calcite percentage above 3.6% (dashed red line) would result in a signal equal to the RMI seasonality (1.5°C) calculated in Table 1. The black star indicates the sample at 454 mm depth which did not detect any calcite. The top of the core is at 0 mm with core age decreasing to the right with increasing depth. Higher values for Mg/Ca, Mn/Ca, and Ba/Ca at the top of the core are due to the tissue layer which is highlighted in cyan (Sayani et al., 2021; Weerabaddana et al., 2021; Wu et al., 2021).

an accelerating voltage of 15.0 KV. All SEM images in this study are secondary electron images taken in greyscale at various magnifications (Figure 1 and Figure S4 in Supporting Information S1).

Phase identification of calcite and aragonite in coral powder samples from MAJ18-2 was conducted using a D8 Advance X-ray diffractometer (Bruker Analytical X-ray Systems, Inc.) at the Department of Geosciences, University of Arizona (Figure S3 in Supporting Information S1). We used zero-background sample holders to improve the signal-to-noise ratio and enhance the low calcite peak resolution that is characteristic of samples with <2% calcite. Samples from observed geochemically altered sections of the coral, areas where trace elemental variability was larger than could be explained by temperature alone, and samples with low δ^{18} O values (indicating

WEERABADDANA ET AL. 6 of 19

warm temperatures or potential calcite diagenesis) were initially selected for XRD analysis. Additional samples containing cold anomalies were also analyzed to ensure we were not biased by selecting only warm peaks of the δ^{18} O record. All coral micro-samples were carefully ground to a fine powder and homogenized using a mortar and pestle. To avoid contamination, the mortar and pestle were cleaned with 2% HNO₃ and deionized water between every sample. A ~7.5 mg aliquot of each sample was weighed using a microbalance ($\pm 10~\mu g$). Weighed samples were then sieved using 50 μm sieve papers directly over the zero-background XRD sample holders to obtain a thin, evenly spread layer of coral powder. Loaded sample holders were set to spin while analyzing to enable maximum spatial exposure of the powder sample to X-rays. Coral powder samples were analyzed using Cu K α radiation over a scanning axis from 25° to 55° (diffraction angle, °2 θ), changing by 0.01° every three seconds (see Figure S3 in Supporting Information S1 for examples of diffraction patterns). Phase identification and quantification of calcite and aragonite in each sample were performed using Rietveld refinement of powder XRD data in Profex 5.0.0 (Doebelin & Kleeberg, 2015).

A laboratory-prepared standard with known amounts of inorganic calcite (2%) and pure coral aragonite (98%) was repeatedly analyzed to demonstrate the accuracy and reproducibility of micro XRD to detect the known trace calcite fraction. The finetuned micro-sample loading technique for XRD was achieved after multiple sensitivity test experiments and is described in detail in Supporting Information S1 (see Text S1 and Table S1 in Supporting Information S1).

We performed an interlaboratory comparison to test the accuracy of our XRD analysis in detecting trace calcite in corals. Coral standards containing 2%, 5%, and 10% weight fractions of calcite were prepared and analyzed using our micro-sample XRD method at the University of Arizona and the Department of Mineral Sciences, Smithsonian National Museum of Natural History (NMNH) (see Table S2 in Supporting Information S1 for results). Note that the NMNH used a different instrument, sample loading technique, and Rietveld refinement software. The XRD analysis performed at NMNH utilized a Rigaku D/Max rapid micro-X-ray diffractometer that uses Debye-Sherrer geometry and Mo K α radiation at 50 kV and 40 mA from 8 to 44° 2 θ . The same coral standard powder samples were loaded into Kapton capillary tubes with a 1 mm inner diameter and capped at the ends using clay dough. Each capillary tube with the sample was fixed and centered at the 0° omega position and spun around phi at 1° per second. Three replicates from each sample were analyzed for 10 and 20 min separately to check for the independence of the exposure time on the result (refer to Farfan et al. (2021, 2023) for more details on the XRD method and Rietveld analysis). The phase fraction of calcite and aragonite in each coral standard sample was quantified with full-pattern Rietveld refinements using GSAS-2 software (Toby & Von Dreele, 2013). Results from both laboratories were compared to determine the accuracy and precision of the calcite measurement using XRD with the modified micro sample loading technique. (Table S2 in Supporting Information S1).

2.5. Statistical Analysis

We analyzed splits of each micro-milled coral powder sample for its calcite percentage and geochemistry. The XRD total uncertainty ($\pm 0.33\%$) we report is the sum of root mean square errors, an additive error of the mean standard deviation of the XRD measurements on 2% calcite standard, and the bias (the difference from the known value). The geochemistry of micro samples was regressed with corresponding percent calcite using weighted least square (WLS) regression to determine the effect of calcite diagenesis on geochemistry. Similarly, δ^{18} O, Sr/Ca, Li/Ca, and Li/Mg were calibrated against SST ERSST v5 using WLS regression (Section 2.3 and Figure S5 in Supporting Information S1). The proxy-calcite regression slope was divided by the proxy-SST regression slope to obtain the temperature sensitivity of each SST-proxy to 1% calcite (Table S3 in Supporting Information S1). Student *t*-test was used to determine the significance of the slopes of regression analyses. We have excluded samples from the tissue layer for statistical analyses where the tissue layer (highlighted in cyan in Figure 2) can have a high concentration of certain trace metals. The significance of all statistical tests in this study is given at a 95% confidence interval (p < 0.05) unless otherwise noted.

We modeled expected coral $\delta^{18}O$ (pseudocoral) as a function of SST and $\delta^{18}O$ of seawater ($\delta^{18}O_{sw}$) using methods described in Thompson et al. (2011). Since the net surface freshwater flux, thus $\delta^{18}O_{sw}$ directly affects SSS and $\delta^{18}O_{coral}$ (Fairbanks et al., 1997; LeGrande & Schmidt, 2006), we used a gridded data set of SSS for tropical Pacific (Delcroix et al., 2011) to estimate $\delta^{18}O_{sw}$ by using slopes of LeGrande and Schmidt (2006). HadISST v1.1 SST (Rayner et al., 2003) was used as input of temperature in the forward model. Annual anomalies (April–March) of coral $\delta^{18}O$ were calculated in MATLAB for the time interval that spans MAJ18-2

WEERABADDANA ET AL. 7 of 19



10.1029/2023PA004730

starting from 1950 (refer to Thompson et al. (2011), Reed et al. (2022), and Thompson et al. (2022) for more details and equations of forward modeling).

3. Results

According to the age model, the MAJ18-2 coral record spans from March 1947–October 1995. Visual inspection of the X-radiograph does not show any areas of potential diagenesis, as identified by dark areas with higher density in positive X-radiographs (McGregor & Gagan, 2003). Critically, the top and the bottom of the coral sampled for geochemistry, where diagenesis is likely to occur in sub-aerially exposed corals, are clear of any dark bands in the X-radiograph (Figure S2 in Supporting Information S1).

3.1. Diagenesis as Seen in SEM

The composition of most of the MAJ18-2 coral skeleton is pristine aragonite. However, there are a few areas where diagenetic textures are present. SEM images show that the top of the core (core depth 15–30 mm) contains a few patchy calcite outgrowths in porous spaces among the pristine aragonite skeleton (Figure 1a). The visual estimate of the percentage coverage of calcite at the top of the coral is <5%. In contrast, core depths between 80 and 115 mm are extensively embedded with calcite outgrowths, with an estimated percentage coverage of ~25% or less (Figures 1d and 1e). Apart from the top and altered sections of the coral, we did not find calcite in any other sections. SEM images show a clear difference between the skeletal texture of the pristine and altered section of the coral (Figure 1). In the middle of the altered section (core depths of 110–115 mm), there is evidence of dissolution at the edges of pore spaces (Figures S4a and S4b in Supporting Information S1). Nevertheless, every core section we examined using SEM shows fine micro-boring tracks on the skeletal surface and these burrows lead to areas of partial dissolution of different levels of severity, which are difficult to quantify (see Figure 1h). In particular, the same coarse texture of partial dissolution is widely present near the bottom of the coral between core depths of 795–800 mm (Figures 1g–1i and Figure S4 in Supporting Information S1). However, there is no evidence of the presence of secondary aragonite in any of the core sections we analyzed with SEM.

3.2. Calcite Distribution in the Coral Skeleton

Calcite percentages in the coral range from 0% to $12.5\% \pm 0.33\%$ (Figure 2). The percent calcite at the top of the core (core depths of 15–30 mm) is less than 2%. Higher calcite percentages (3%–12.5%) are present within the diagenetically altered section of the coral starting from a core depth of 56 mm, where we see offsets from the mean geochemistry of most proxies (highlighted in gray in Figure 2). Calcite percentages drop back to below 2% after the core depth of 155 mm, marking the end of the diagenetic alteration. Calcite percentages at core depths below the diagenetic area of the coral never exceed 3% except for samples at depths of 187 mm (3.8%), 219 mm (4.1%), and 250 mm (4.1%).

Except for δ^{18} O, the WLS relationships between SST-sensitive proxies and measured percent calcite are significant at a 99% confidence interval (Li/Ca, r = -0.49; Li/Mg, r = -0.62; Sr/Ca, r = -0.52; n = 34) (Figure 3, Table 1). Values of Li/Ca, Li/Mg, and Sr/Ca decrease with increasing calcite percentage, giving rise to warmer-than-expected reconstructed temperatures. The relationship between percent calcite and Mg/Ca and B/Ca is significant at a 95% confidence interval, whereas U/Ca is significant at a 90% confidence interval. Finally, the Ba/Ca and Mn/Ca-calcite relationship is not significant, indicating the least effect of calcite on these proxies (Figure 3).

We calculate the sensitivity of each temperature proxy to intra-skeletal calcite in MAJ18-2, based on the slopes of proxy-SST calibrations and proxy-calcite regression (Table 1 and Figure S5 in Supporting Information S1). Among the analyzed SST proxies, Sr/Ca is the most sensitive (0.41°C per 1% calcite) and δ^{18} O is the least sensitive (0.008°C per 1% calcite) proxy for intra-skeletal calcite diagenesis. We do not assess Mg/Ca and U/Ca as temperature proxies in this study because they are only indirectly related to temperature and are strongly influenced by local climatology and marine carbonate chemistry (Corrège, 2006; DeCarlo et al., 2015; Min et al., 1995; Wei et al., 2000). Additionally, we calculate the calcite percentage that produces temperature departures that are equivalent to RMI seasonality (1.5°C) to set the minimum threshold for screening altered samples for temperature reconstruction. A calcite percentage above 3.6% can significantly affect Sr/Ca-SST-based paleoclimate reconstruction in MAJ18-2 (Table 1 and Figure 2). Minimum screening levels when Li/Ca-SST is used is about twice that of Li/Mg-SST because Li/Mg is more sensitive to calcite than Li/Ca by about a factor of two (Table 1).

WEERABADDANA ET AL. 8 of 19

25724525, 2024, 5, Downloaded from https://agupubs.onlinelibrary.wiley.com/doi/10.1029/2023PA.004730 by University Of Arizona Library, Wiley Online Library on [03/05/2024]. See the Terms and Conditions (https://agupubs.onlinelibrary.wiley.com/doi/10.1029/2023PA.004730 by University Of Arizona Library, Wiley Online Library on [03/05/2024]. See the Terms and Conditions (https://agupubs.onlinelibrary.wiley.com/doi/10.1029/2023PA.004730 by University Of Arizona Library. Wiley Online Library on [03/05/2024]. See the Terms and Conditions (https://agupubs.onlinelibrary.wiley.com/doi/10.1029/2023PA.004730 by University Of Arizona Library.

on Wiley Online Library for rules of use; OA articles are governed by the applicable Creati

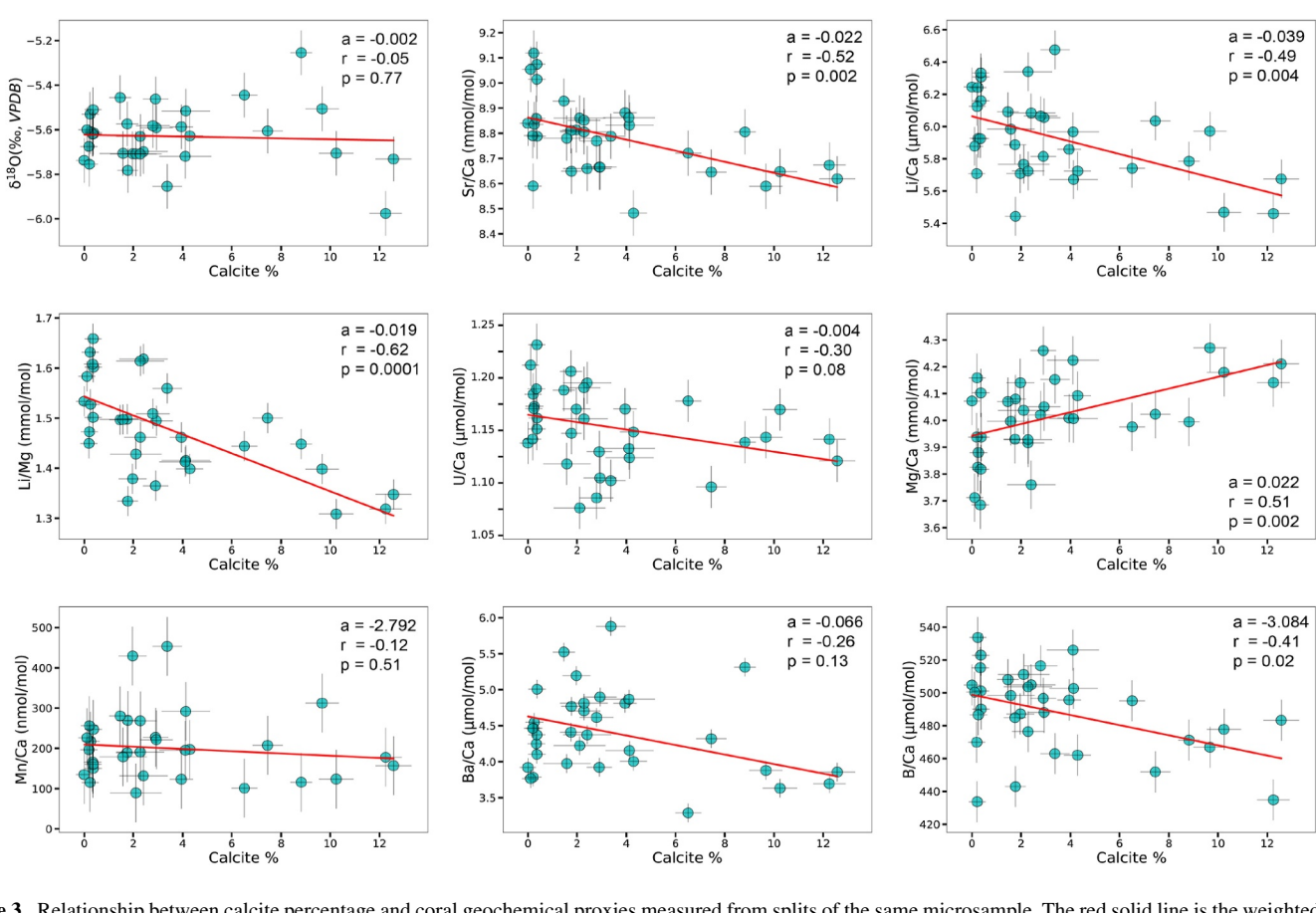


Figure 3. Relationship between calcite percentage and coral geochemical proxies measured from splits of the same microsample. The red solid line is the weighted least square regression. Slope (*a*), correlation coefficient (*r*), and *p* values are given inside each regression plot.

3.3. Reconstructed SST

Removing the diagenetic section containing higher calcite percentages improves the reconstructed SST (SSTr) (Table S3 in Supporting Information S1). The median SSTr for each proxy is not significantly different from the average of the gridded ERSST (28.62°C) when the diagenetic section is removed (i.e., without diagenesis or "WoD" in Table S3 in Supporting Information S1). The maximum temperatures (Max in Table S3 in Supporting Information S1) of all SSTr reduce and are close to the observed maximum SST (29.77°C of the ERSST) when the diagenetic section is removed (WoD in Table S3 in Supporting Information S1). In contrast, the minimum temperatures (Min in Table S3 in Supporting Information S1) of all SSTr remain unchanged regardless of removing the diagenetic section, and the minimum of the SSTr for Sr/Ca is critically lower than the minimum of all SSTr and gridded ERSST (Table S3 in Supporting Information S1).

Table 1Temperature-Proxy Sensitivity to Percent Calcite in the Coral

Y				
Temperature proxy sensitivity	$\delta^{18}O$	Sr/Ca	Li/Ca	Li/Mg
Proxy-SST calibration slope (°C ⁻¹)	-0.252	-0.051	-0.367	-0.080
Proxy-calcite calibration slope (per 1% calcite)	-0.002	-0.022	-0.039	-0.019
Temperature-proxy-calcite sensitivity (°C per 1% calcite)	+0.008	+0.431	+0.106	+0.238
Calcite threshold equivalent to RMI seasonality (1.5°C)	190%	3.6%	14.1%	6.3%

Note. Units of δ^{18} O, Sr/Ca, Li/Ca, and Li/Mg are ‰, mmol/mol, µmol/mol, and mmol/mol, respectively. The 1.5°C seasonality at the RMI was calculated using ERSST data as the difference between average summer and winter temperatures. Calibration slope values in italics are significant at a 99% confidence interval and in both bold and italics are significant at a 99.99% confidence interval.

WEERABADDANA ET AL. 9 of 19

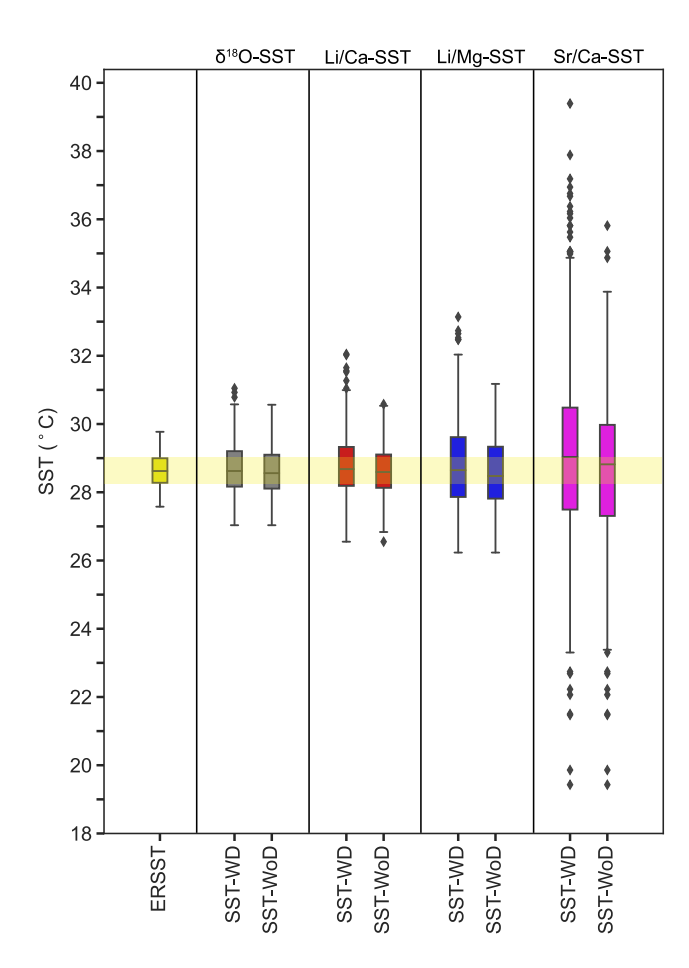


Figure 4. Box plot distribution of ERSST and reconstructed SST (SSTr) from MAJ18-2 coral δ^{18} O, Li/Ca, Li/Mg, and Sr/Ca for the time interval 1947–1995. SSTr distribution for each proxy is compared to ERSST when including the diagenetically altered section (given under SST-WD) and after removing the altered section (given as SST-WoD). The band highlighted in yellow indicates the range of ERSST across other proxy-based SSTr ranges.

Applying the local proxy-temperature calibration to all robust temperature proxies (see Figure S5 in Supporting Information S1 for calibration plots), all SSTr skew positively toward warm temperatures before removing the diagenetically altered section. However, this bias decreased after removing the altered section and even became cold-biased for Sr/Ca-SST (see skewness in Table S3 in Supporting Information S1). All SSTr are warm biased before removing the altered section, with SSTr values that were anomalously greater than the observed SST (SST-WD in Figure 4). This warm bias either decreased or completely removed after excluding data from the diagenetic section (SST-WoD in Figure 4). SSTr from Sr/Ca indicates a wide range when compared to the range of ERSST on both warm and cold sides of the distribution. The cooler end of the SSTr of Sr/Ca is exceptionally lower than that of the observed SST, with a remaining cold bias that is not removed by excluding the diagenetic section (see Figure S6 in Supporting Information S1 for a Q-Q plot of the same data against a normal distribution for further clarification).

4. Discussion

4.1. Intra-Skeletal Calcite Diagenesis

The calcite percentages measured by XRD in individual micro samples and estimated from SEM images show that MAJ18-2 is mostly pristine. Many warm peaks we analyzed in the $\delta^{18}O$ record (low $\delta^{18}O$ values) had low calcite percentages. This suggests that the majority of the warm peaks represent the actual climatology. Most cold peaks we analyzed also had low percent calcite (<1%), suggesting that we have not biased the results in selecting predominantly warm peak samples from the $\delta^{18}O$ record for XRD analysis.

Euhedral blocky crystals of calcite observed in SEM images (Figure 1) along with XRD, confirm calcite precipitation in the altered section of the coral (Longman, 1980; McGregor & Gagan, 2003; Sayani et al., 2011). Similar to a vadose zone, the dissolution of aragonite due to meteoric water facilitates ion leeching and recrystallization to form other polymorphs of CaCO₃, such as calcite, that change the original geochemical signature (James, 1972). Calcite precipitation starts from a diagenetic front where a thin layer of undersaturated

meteoric water dissolves the surface aragonite layer which over time, saturates this fluid with CaCO₃ and drives inorganic calcite precipitation (James, 1972, 1974a; McGregor & Gagan, 2003). A chalky texture appears due to partial dissolution, which provides nuclei for calcite precipitation (James, 1974a; Marshall, 1983); this may explain the rough primary surfaces seen in the diagenetic section (Figure 1 and Figure S4 in Supporting Information S1).

4.2. Improvements in Quantifying Percent Calcite Using XRD

The new sample loading technique we use for XRD analysis significantly constrains the uncertainty of calcite quantification estimates and the sample size required for the detection of low-level calcite diagenesis using the standard XRD method. An inter-laboratory comparison of XRD methods showed that our results are in good agreement with the results from the Smithsonian NMNH, showing the reproducibility of Rietveld analysis within analytical uncertainty (Table S2 in Supporting Information S1). The total uncertainty of XRD for percent calcite $(\pm 0.33\%)$ is significantly lower than previous studies that report uncertainties of $\pm 2\%$ –7% (Lazareth et al., 2016; McGregor & Abram, 2008; McGregor & Gagan, 2003). A low percent error in our method enables accurate measurement of trace-calcite $(\sim 1\%)$ that is otherwise not detected. Based on the visual detection of the calcite peak in the XRD spectra, we will consider a conservative value between 0.37% and 0.89% (ideally above 0.50%) as the limit of detection of calcite in this study (see Figure S3 in Supporting Information S1 for clarification). Additionally, the weight of the coral powder sample used for XRD $(\sim 7.5 \text{ mg})$ is significantly lower than similar studies that require $\sim 200 \text{ mg}$ or more (Lazareth et al., 2016; McGregor & Gagan, 2003; Sayani et al., 2011). Moreover, we produced straightforward, easily interpretable results regarding the impact of calcite on

WEERABADDANA ET AL. 10 of 19



10.1029/2023PA004730

geochemistry. By analyzing splits of the same micro-milled sample (collected at 1.0 mm intervals along a transect) for geochemistry and XRD, we facilitate a direct comparison of the effect of calcite diagenesis on the geochemical signatures of individual data points for paleoclimate reconstruction. To our knowledge, this is the first time analyzing the impacts of calcite diagenesis on the geochemistry of the same sample at a millimeter scale; previous work has focused on bulk sample analysis that typically compares averages over a few centimeters of the coral (Lazareth et al., 2016; McGregor & Gagan, 2003; Sayani et al., 2011).

4.3. Implications of Intra-Skeletal Calcite on Coral Geochemistry

4.3.1. Coral Sr/Ca

Sr/Ca values in samples from the diagenetically-altered section are comparatively lower than the non-diagenetic section of MAJ18-2. This is consistent with less Sr^{2+} incorporation into the calcite phase, mediated by the distinct partitioning coefficients of Sr^{2+} in the calcite (0.13) and aragonite (1.6) phases (Veizer, 1983). When compared with the orthorhombic aragonite crystal structure, the rhombohedral calcite crystal structure can accommodate less Sr^{2+} replacing Ca^{2+} (Sayani et al., 2011). Consequently, corals that undergo calcite diagenesis experience a change in the distribution of trace elements compared to the original aragonite skeleton, with implications for thermodynamically derived trace element-temperature relationships. The average value of Sr/Ca in the diagenetic section is 0.22 mmol/mol less than the rest of the well-preserved coral, with extreme Sr/Ca values as low as 8.31 mmol/mol reported in the diagenetic section (average Sr/Ca in the non-diagenetic section was 8.88 mmol/mol), causing a mean shift in the Sr/Ca seasonal cycle (highlighted in Figure 2).

A few samples with high Sr/Ca values were also analyzed below the diagenetic section of the coral. The values of these samples reached up to 9.37 mmol/mol, which is significantly different from the average Sr/Ca of the coral. Secondary aragonite can increase Sr/Ca values up to 10 mmol/mol or above (Rashid et al., 2020). These higher values are still less than Sr/Ca values commonly observed in aragonite cement (>10.0 mmol/mol in Allison et al. (2007)) and no secondary aragonite was observed in SEM imagery.

A considerable level of diagenesis caused by partial dissolution in our coral may have resulted in lower Sr/Ca values observed at discreet intervals (Figure S4 in Supporting Information S1). We observed partial dissolution and chalky textures in the skeleton of the altered section and in each core section we analyzed for SEM, especially in areas having microboring animal tracks (shown in Figure S4 in Supporting Information S1). These micro pathways provide passage for meteoric water to flow into the coral and start dissolving the primary aragonite skeleton. Studies have shown that dissolved surfaces with chalky textures are still aragonitic and have not transformed into calcite (James, 1974b). Dissolution starts from the centers of calcification (CoC) and expands in an inside-out pathway. CoC primarily contains higher Sr/Ca, thus leaving areas with low Sr/Ca surfaces during dissolution (Allison & Finch, 2004). Thus, measured Sr/Ca from such areas may have lower Sr/Ca ratios that are typical of dissolution, suggesting that the high Sr/Ca anomalies observed in the core may not be due to diagenesis. Further, we did not observe a relationship between areas of dissolution and geochemical anomalies.

Finally, to confirm that organic matter content is not contributing to the geochemical offsets, we performed the lost-on-ignition (LOI) test on seven samples (three from the diagenetically altered section and four from the pristine section of MAJ18-2) and quantified the amount of organic content in each sample (refer to Text S2 in Supporting Information S1 for methods). The LOI test results do not infer a significant difference in organic matter content among those seven samples (Table S7 in Supporting Information S1), thus suggesting that observed geochemical offsets are not due to different organic matter content. We, therefore, focus the remainder of our discussion on the section on calcite diagenesis and its implications on climate reconstruction.

4.3.2. Coral Li/Ca, Mg/Ca, and Li/Mg

The diagenetic section containing intra-skeletal calcite has significantly less Li/Ca and Li/Mg than the rest of the well-preserved coral. Li⁺ and Mg²⁺ are also substituted into the aragonite skeleton by replacing Ca²⁺ when forming aragonite skeleton and the original concentrations can be impacted by both dissolution and reprecipitation of secondary materials such as calcite. In contrast to Ca^{2+} substitution by Sr^{2+} , inorganic precipitation experiments suggest a heterovalent substitution (substituting ions with different valences) of Ca^{2+} by two Li ⁺ into the aragonite crystal structure of coral skeletons (Hathorne, Felis, et al., 2013; Marriott et al., 2004). Calcite accommodates less Li⁺ in its structure (two Li⁺ take more space than one Ca^{2+}). Therefore, we expected lower

WEERABADDANA ET AL. 11 of 19

Li/Ca values in the diagenetic section with more calcite and found that the average Li/Ca in the diagenetic section (5.67 μmol/mol) is indeed lower than in the non-diagenetic section (6.22 μmol/mol).

Mg/Ca significantly increased in the diagenetically-altered, calcite-rich section when compared to the non-altered section of the coral (Figure 2). This is evident from the positive relationship between Mg/Ca and percent calcite (r = 0.51, n = 34; Figure 3). During secondary calcite diagenesis, the calcite phase is enriched in Mg²⁺ due to a higher partitioning coefficient of Mg in calcite relative to aragonite (Rabier et al., 2008). This mechanism explains the greater coral Mg/Ca concentration in the diagenetic section, with values reaching up to \sim 4.4 mmol/mol in this section (i.e., greater than the core average of 3.9 mmol/mol). The incorporation of Mg²⁺ into the aragonite skeleton is indirectly driven by temperature via changes in coral physiology and the rate of precipitation of the skeleton (DeCarlo et al., 2015; Inoue et al., 2007; Reynaud et al., 2007). This makes Mg/Ca measured in diagenetically altered sections of the coral more complex as the dissolution phase in the vadose zone may contain a combination of different origins of Mg concentrations. Thus, we expect Mg/Ca in calcite to vary on a case-by-case basis and this relationship needs to be more closely investigated.

Using Mg/Ca to remove the non-temperature signal from Li/Mg, we find that the "robust" Li/Mg paleothermometer also displays a significant, strong negative correlation with calcite percentage (r = -0.61, n = 34). This is consistent with the reduced Li/Mg reported by Lazareth et al. (2016). We, therefore, expected Li/Mg in the diagenetic section to be lower, considering the higher percent calcite (up to 12.5%) detected in the diagenetic section. Li/Mg values in the diagenetic section are lower than in the non-diagenetic section, but only by 0.18 mmol/mol. The mechanism of both heterovalent Mg²⁺ and monovalent Li⁺ precipitation in the calcite phase is not well studied; more work is therefore needed to understand how leeching from primary aragonite and reprecipitation in calcite causes less Li/Mg to be present in calcite.

4.3.3. Coral B/Ca and U/Ca

B/Ca has a significant correlation with percent calcite (r = -0.42, n = 34), with less boron incorporation into the calcite phase. This observation is consistent with Griffiths et al. (2013) that showed a similar reduction in B/Ca in the presence of calcite. The process of biomineralization can be affected by both biological and physical stressors that contribute to different skeletal ion concentrations (Tambutté et al., 2011). However, corals can modify the chemistry of their semi-enclosed calcifying fluid by actively increasing its pH and increasing the diffusion of ions such as boron into the polyp (Holcomb et al., 2016). In contrast, changes in the concentration of such ions during diagenetic skeletal dissolution and reprecipitation into calcite or aragonite are regulated by varying dissociation constants based on the concentration of the solution phase and temperature. Consequently, subaerial precipitation of secondary material such as calcite incorporates less boron due to varying precipitation rates and speciation during phase change, which modifies the original concentrations in the aragonite skeleton (Mavromatis et al., 2015). Uranium partitioning between seawater and aragonite depends on temperature, pH, and carbonate ion concentration while U/Ca measured in aragonite skeleton is a function of these factors (DeCarlo et al., 2015). Dissolution and phase change from aragonite to calcite during diagenesis alters the original uranium concentration thus changing the original signal. We also found lower U/Ca values in the calcite-rich diageneticallyaltered section of the coral, which contradicts previous studies that observed greater U/Ca in high Mg-calcite (Allison et al., 2007; Gvirtzman et al., 1973). This discrepancy may reflect differences between intra-skeletal calcite (this study) and calcite cement (their studies), which have slightly different partition coefficients and preferred phases (high Mg-calcite vs. calcite). Therefore, the type of calcite precipitated because of diagenesis is also important to interpret changes in geochemistry.

4.3.4. Coral Ba/Ca and Mn/Ca

Episodic proxies, such as Ba/Ca and Mn/Ca, exhibit different yet insignificant relationships with intra-skeletal calcite. Ba/Ca is negatively related to percent calcite (r = -0.27, n = 34). Ba/Ca concentration in the diagenetic section is reduced by 0.44 µmol/mol when compared to the rest of the non-diagenetic section of the coral. However, the sensitivity of Ba/Ca to calcite diagenesis is -0.06 µmol/mol per 1% calcite, which is less than the reported error of the Ba/Ca measurement in this study (0.137 µmol/mol, 2σ). Therefore, the effect of less than \sim 2% calcite on Ba/Ca measurement is not detectable. Similarly, the slope of Mn/Ca and percent calcite regression is not significant and suggests that the effect of calcite on Mn/Ca is minimal. The error in the Mn/Ca measurement

WEERABADDANA ET AL. 12 of 19

is also large enough to mask the effect of low levels of calcite (Table S5 in Supporting Information S1), so we do not expect to see a noticeable effect on Mn/Ca from intra-skeletal calcite in the diagenetic section.

4.3.5. Coral δ^{18} O

There is no significant relationship between $\delta^{18}O$ values, and the percent calcite measured in MAJ18-2 (Figure 3). The effect of 1% calcite on $\delta^{18}O$ values was -0.002% (Table 1). The average value of $\delta^{18}O$ in this study is slightly less in the calcite-bearing diagenetically altered section by a value of 0.21%. Still, this difference cannot be explained by diagenesis alone. Thus, the oxygen isotope signature measured in the diagenetic section might be a combination of dissolved oxygen from the aragonite skeleton and oxygen from the meteoric water. If the rate of meteoric water flow is greater than the rate of dissolution in the vadose zone of the coral, there is a higher possibility that the calcite precipitated in the diagenetic zone will represent the $\delta^{18}O$ signature of the meteoric water (O'Neil et al., 1969). Our results suggest that the effect of diagenetic calcite on stable isotopes is much less severe than for trace metals present in the coral in a sub-aerially exposed setting.

4.4. Implications of Intra-Skeletal Calcite on Paleoclimate Reconstruction

4.4.1. Implications for Temperature

Intra-skeletal calcite modifies the primary coral geochemical signal, which is a function of ambient seawater chemistry at the time of coral growth and thus the local paleoclimate conditions. According to our results, δ^{18} O is the temperature proxy that is least affected by calcite diagenesis (Table 1). Thus, δ^{18} O may serve as the most reliable proxy for paleo-temperature reconstruction from sub-fossil corals where diagenesis is common or in areas of any coral core where diagenesis is suspected (Figure 3). However, the average δ^{18} O-SST in the diagenesis section is ~0.9°C warmer than the rest of the well-preserved coral (significantly greater than the ERSST SST difference of 0.17°C, which we explain as true warming during the time period covered by the diagenetic section of the core). However, the mean shift in SSTr from δ^{18} O may not be explained by diagenesis alone, because the δ^{18} O signature in calcite likely incorporates some amount of the δ^{18} O value of meteoric water (Gross, 1964) that percolates into the vadose zone of the coral. The δ^{18} O value measured in an altered coral can reflect a significant contribution of the δ^{18} O signature of meteoric water when the flow rate is greater than the rate of calcite precipitation (which is likely happening in vadose environments in sub-aerially exposed corals). These diagenetic processes can offset the δ^{18} O-SST relationship, which might explain the δ^{18} O-SST offset that we observe in the diagenetic section. Although our results suggest that flow rates at this site minimize the impact of meteoric water on the δ^{18} O values of the secondary calcite, identifying samples containing calcite that can significantly affect temperature reconstruction is still critical for calculating the δ^{18} O-SST relationship and reconstructing robust,

Further, coral δ^{18} O values are a function of SST and δ^{18} O of seawater (which in turn is related to changes in salinity); thus, our SSTr from δ^{18} O does not solely represent SST variability in the RMI. SST and δ^{18} O of seawater covary at our site, amplifying the climate signal recorded in skeletal δ^{18} O (Thompson et al., 2022). Therefore, some of the differences between observed and reconstructed SST from $\delta^{18}O$ can be attributed to $\delta^{18}O$ of seawater and its covariance with SST amplifying the variability relative to SST alone. To address this, we modeled expected coral δ^{18} O values (pseudocorals) using observed SST and sea surface salinity (SSS) following the method described by Thompson et al. (2011). Modeled δ^{18} O anomalies were compared with anomalies of measured δ^{18} O values before and after removing the altered section (Figure S7 in Supporting Information S1). There are negative δ^{18} O anomalies (warm anomalies) present in the coral when the altered section is included (minimum = -0.34 %), and those anomalies disappear after removing the altered section (minimum = -0.16%). The negative skewness of measured δ^{18} O anomalies with diagenesis (-0.90) is also reduced when the diagenetic section is removed (-0.39), consistent with the removal of the warm biased portion of δ^{18} O due to diagenesis (Table S4 in Supporting Information S1). However, the averages of δ^{18} O anomaly with and without the altered section are not significantly different from the pseudocoral anomalies, again emphasizing that δ^{18} O is relatively robust to calcite diagenesis, although the negative bias in the data is removed when excluding the altered section of the coral.

Lower values of Sr/Ca, Li/Ca, and Li/Mg in the diagenetic section of the coral skew SSTr toward high temperatures (warmer than the average) that cannot be explained by the local climatology (Figure 4 and Figure S6 in Supporting Information S1). These results are consistent with δ^{18} O-SSTr, but the degree of effect of calcite on

WEERABADDANA ET AL. 13 of 19

SSTr from each proxy is different. The SST reconstruction based on Sr/Ca is the most sensitive temperature proxy to calcite diagenesis (0.43°C per 1% calcite; Table 1). When converted to SST, the average Sr/Ca-SST, Li/Mg-SST, and Li/Ca-SST in the diagenetic section is ~4.1°C, ~2.25°C, and ~1.5°C warmer than the rest of the well-preserved coral, respectively (again, significantly greater than ERSST warming of ~0.17°C during the time period corresponding to the diagenetic section of the coral). Both Li/Ca and Li/Mg are less sensitive to calcite diagenesis than Sr/Ca (Table 1), thus SST reconstructions based on these two proxies could be more promising in potentially altered subfossil cores. The sensitivity of Li/Mg-SST to calcite in this study (0.24°C per 1% calcite) is comparable to that of Lazareth et al. (2016) (0.26°C per 1% calcite). Finally, the sensitivity of Li/Ca-SST is 0.11° C per 1% calcite, and when converted to Marshall Islands seasonality, it requires 14.1% calcite to exceed the effect of local climatology (~1.5°C). None of our samples had calcite percentages close to this level (maximum was 12.5%). These results suggest that Li/Ca is the best single trace element proxy for SST reconstruction in areas of poor skeletal preservation (Table 1 and Table S3 in Supporting Information S1).

The SSTr from Sr/Ca also displays a negative skew, with cold temperature artifacts that are not present in ERSST SST. The reconstructed minimum temperature from Sr/Ca is 19.23° C which is significantly lower than the ERSST minimum (27.58°C). Even after removing SSTr data from the diagenetic section, the Sr/Ca-SSTr minimum remained unchanged (Table S3 in Supporting Information S1) suggesting that the cold anomalies were not associated with the section having higher calcite percentages (see also Figure 4). SEM images from the diagenetic section and other core sections provide clear evidence of partial dissolution (Figure S4 in Supporting Information S1). Trace elements are susceptible to incongruent leaching through dissolution that can give colder than observed temperatures (Hendy et al., 2007). However, cold temperatures in SSTr from Sr/Ca cannot be explained by the dissolution, as we expect our coral to be relatively enriched in low Sr/Ca surfaces (thus warm biasing SSTr) due to the dissolution of CoC which contains high Sr/Ca (Cohen & McConnaughey, 2003). Further, we do not see a significant cold bias in SSTr from δ^{18} O, Li/Ca, or Li/Mg (Table S3 in Supporting Information S1; Figure 4) in our coral record, or any strong evidence for secondary aragonite in any core section we analyzed for SEM (Figure 1 and Figure S4 in Supporting Information S1).

The application of Sr/Ca as a temperature proxy may be compromised by geology and local climatology (Wei et al., 2000). The seawater chemistry in Majuro Atoll may be influenced by submarine aquifers that drain rainwater through the carbonate basement of the atoll which can compromise the Sr/Ca-temperature relationship (Rahaman et al., 2022). But in this study, we do not have enough evidence to support this argument without further investigation. Other sources of Sr/Ca-SST variability at this site will be investigated in future work, paired with investigations of seawater samples from this site collected from Majuro Atoll since 2016.

We demonstrate that the difference in SSTr with and without diagenesis can be significant even over a short climate record, suggesting that diagenesis is therefore likely to affect multi-centennial climate records. Estimates of subtle SST variability in the tropical oceans can be enhanced due to low percentages of calcite (1%–2%) in subfossils, which was either not detectable using earlier methods or considered as too little to bias temperature. Hence, we recommend corals used in paleoclimate reconstructions should be assessed for trace calcite diagenesis regardless of the length of the time span of the reconstruction. Additionally, we emphasize the importance of micro XRD approaches (or modified loading techniques for traditional XRD, presented here) for accurately identifying calcite percentages and determining the best working proxy for SST at a given location and coral depending on its level of skeletal preservation. We demonstrate that the effect of trace calcite on different temperature proxies varies by its diagenetic nature and the extent of alteration. For example, in our samples, SSTr reconstructed using Li/Ca accounts for lesser diagenetic effects by calcite than when using Sr/Ca. Therefore, the accuracy of paleoclimate interpretation from a diagenetically altered coral can be improved based on the choice of the coral proxy.

4.4.2. Implication for Other Proxy-Based Paleoclimate Reconstructions

B/Ca is a proxy for carbonate chemistry of the coral calcifying fluid (especially dissolved inorganic carbon, DIC) and is often used to reconstruct calcifying fluid pH when combined with δ^{11} B (Holcomb et al., 2016). Diagenetic effects on B/Ca can compromise the seawater carbonate chemistry and pH reconstruction that are important to understand changes in coral biomineralization. Previous studies have shown that increasing the percent calcite reduces δ^{11} B (Lazareth et al., 2016), suggesting that the boron isotopic fractionation between precipitating solution and calcite lattice is modified during diagenetic incorporation of B/Ca. Boron in seawater exists as either

WEERABADDANA ET AL. 14 of 19

boric acid [B(OH)₃] or borate [B(OH₄)⁻] depending on the pH of the seawater (Zeebe, 2005). Borate ion concentration in seawater is modified inside the semi-isolated calcifying fluid during carbonate ion upregulation (with the calcifying fluid is enriched in carbonate ions relative to seawater) and can be co-precipitated into the skeleton in place of the carbonate ion during calcification (Al-Horani et al., 2002; McCulloch et al., 2012). Such modifications in the chemistry of the calcifying fluid help modify the carbonate saturation state to readily precipitate the aragonite skeleton (Farfan et al., 2018; Holcomb et al., 2016; Tambutté et al., 2011). Because of this biogenically-mediated elevation of boron in the calcifying fluid, we expect B/Ca values to be significantly reduced by inorganically-precipitated, secondary calcite; indeed, we identify a significant relationship between percent calcite and B/Ca, with lower B/Ca in intra-skeletal calcite (Figure 3). Therefore, caution is needed in interpreting the decreased B/Ca in the diagenetic section to avoid wrong interpretations about changes in the carbonate chemistry of the calcifying fluid and seawater.

Mg/Ca incorporation into the aragonite crystal structure is indirectly influenced by temperature via its response to coral calcifying fluid dynamics and coral extension rate (DeCarlo et al., 2015; Inoue et al., 2007; Reynaud et al., 2007). Hence, Mg²⁺ concentration in the solution phase of a diagenetic front can have a mixture of different aragonite skeletal Mg imprints due to varying environmental conditions including SST. Thus, it becomes more complex to interpret Mg/Ca when calcite is present, and it is best to avoid using such proxies in the presence of intra-skeletal calcite diagenesis. Nevertheless, Mg/Ca is not considered a robust temperature proxy but can be used in understanding biomineralization under various stressors and is important to fine-tune the behavior of other trace elements during coral skeletogenesis (DeCarlo et al., 2017).

The impact of intra-skeletal calcite on U/Ca is not significant enough at low levels of diagenesis to cause distinct changes in paleo-reconstructions. Early studies have used U/Ca as a proxy for SST (Min et al., 1995); assuming a direct temperature effect, we expect warm temperature artifacts deduced from U/Ca due to calcite diagenesis $(-0.004 \ \mu mol/mol)$ per 1% calcite). The estimation of temperature sensitivity of U/Ca can be $+0.09^{\circ}$ C per 1% calcite (based on the calibration of Sinclair et al. (1998); $-0.046 \ \mu mol/mol/^{\circ}$ C for *Porites*). However, recent experimental studies have found that the incorporation of uranium into the skeleton is a direct effect of carbonate ion concentration in the calcifying fluid (DeCarlo et al., 2015). This relationship can only be partly explained by either pH or temperature; therefore, the use of U/Ca as a robust temperature proxy is questionable. Nevertheless, the effect of diagenesis on U/Ca will impact estimates of calcifying fluid geochemistry. Additionally, avoiding calcite diagenetic sections in corals is important when selecting samples for U-series dating where secondary calcite can otherwise modify the age of a coral.

Reduced Ba/Ca in diagenetic areas containing intra-skeletal calcite could be wrongly interpreted as times of reduced upwelling or rainfall. According to our Ba/Ca-calcite calibration, the presence of 10% calcite would reduce the average Ba/Ca by $0.6~\mu$ mol/mol. In comparison, most of the coral Ba/Ca studies have reported Ba/Ca variability of less than $12~\mu$ mol/mol (exceptionally reaching values above $20~\mu$ mol/mol) (refer to Weerabaddana et al. (2021) for a summary of Ba/Ca studies). Therefore, interpreting coral Ba/Ca from a diagenetically altered coral depends on the Ba/Ca variability (i.e., signal) at a given location for a specific coral species and the extent of calcite diagenesis (i.e., noise).

The effect of calcite diagenesis on coral Mn/Ca is first reviewed in this study. There is a slight decrease in Mn/Ca in the presence of calcite (3.3 μ mol/mol per 1% calcite; Figure 3), but this relationship is not significant. When considering the large Mn/Ca variability in our coral (average = 200 μ mol/mol), the effect of intra-skeletal calcite on Mn/Ca is negligible over typical range of trace calcite diagenesis observed. We observed many Mn/Ca peaks that are above 200 μ mol/mol baseline and are characteristic of westerly wind events in the tropical Pacific (Sayani et al., 2021). Resuspended Mn²⁺ in the seawater during tropical Pacific westerly wind events can be incorporated into the coral skeleton as a function of the wind stress (Kojima et al., 2022; Thompson et al., 2015). Nevertheless, the enrichment of Mn²⁺ concentration in seawater can vary by location, the depth of the lagoon, and the intensity of trade winds (Kojima et al., 2022). Hence, both local climatology and the level of calcite diagenesis in corals should be considered when using Mn/Ca as a proxy for trade winds, though our results suggest that this proxy is likely robust to typical levels of diagenesis.

5. Conclusion

Although fine-scale diagenetic alterations are not visible in X-radiographs, intra-skeletal calcite has varying degrees of impact on commonly utilized geochemical proxies. Our study emphasizes the importance of

WEERABADDANA ET AL. 15 of 19

prescreening corals used in paleoclimate studies at mm-scale resolution to identify diagenesis and to determine the best working proxy for temperature reconstruction based on the level of skeletal preservation. Trace levels of calcite (~1%–2%) in corals can bias temperature reconstructions, exaggerating seasonal climatology and internal climate variability in tropical locations. Identifying and removing data from the diagenetically altered section can greatly improve the confidence of paleoclimate reconstructions. However, in doing so we might miss either critical spatial or temporal data from the climate record. If the level of diagenesis is quantified and proxy-calcite sensitivity is well-calibrated on individual samples (as in this study), proper calibrations may be applied to account for approximate non-climate artifacts to refine paleoclimate reconstructions and expand the spatial and temporal coverage of paleoclimate data. We suggest that micro powder XRD is a useful method that should be further utilized to detect low-level diagenesis and improve paleoclimate reconstruction across the global tropics and beyond.

Conflict of Interest

The authors declare no conflicts of interest relevant to this study.

Data Availability Statement

All data presented in this study are archived and publicly available via the NOAA NCEI Paleoclimatology database repository and can be accessed via Weerabaddana et al. (2023). NOAA Extended Reconstructed Sea Surface Temperature V5 (ERSSTv5) data (Huang et al., 2017) can be downloaded at http://iridl.ldeo.columbia.edu/SOURCES/.NOAA/.NCDC/.ERSST/.version5/.sst/. Hadley Center Sea Ice and Sea Surface Temperature (HadISST v1.1) data (Rayner et al., 2003) can be downloaded at https://www.metoffice.gov.uk/hadobs/hadisst/data/download.html. Profex 5.0.0 open source XRD and Rietveld refinement software (Doebelin & Kleeberg, 2015) can be downloaded at https://www.profex-xrd.org/. GSAS-2 software used for Rietveld analysis of XRD patterns (Toby & Von Dreele, 2013) can be downloaded at https://subversion.xray.aps.anl.gov/trac/pyG-SAS, available via open source license https://subversion.xray.aps.anl.gov/pyGSAS/trunk/license2013.txt. JCp-1 data in Table S5 in Supporting Information S1 is from Hathorne, Gagnon, et al. (2013).

Acknowledgments

This work is supported by NSF-CAREER-1945479 (to D.M.T). We thank Bob Downs for facilitating XRD analysis and Zachary Michels at the University of Arizona LaserChron Center for helping to take SEM images of corals. We also thank Luz Romero for helping with trace metal analysis in our coral samples. We thank anonymous reviewers, Marcus Lofverstrom and Kaustubh Thirumalai for their feedback and suggestions to improve the manuscript.

References

- Al-Horani, F. A., Al-Moghrabi, S. M., & de Beer, D. (2002). The mechanism of calcification and its relation to photosynthesis and respiration in the scleractinian coral *Galaxea fascicularis*. *Marine Biology*, 142(3), 419–426. https://doi.org/10.1007/s00227-002-0981-8
- Allison, N., & Finch, A. A. (2004). High-resolution Sr/Ca records in modern *Porites lobata* corals: Effects of skeletal extension rate and architecture. *Geochemistry, Geophysics, Geosystems*, 5, Q05001. https://doi.org/10.1029/2004gc000696
- Allison, N., Finch, A. A., Webster, J. M., & Clague, D. A. (2007). Palaeoenvironmental records from fossil corals: The effects of submarine diagenesis on temperature and climate estimates. *Geochimica et Cosmochimica Acta*, 71(19), 4693–4703. https://doi.org/10.1016/j.gca.2007.07.026
- Bar-Matthews, M., Wasserburg, G., & Chen, J. (1993). Diagenesis of fossil coral skeletons: Correlation between trace elements, textures, and 234U238U. *Geochimica et Cosmochimica Acta*, 57(2), 257–276. https://doi.org/10.1016/0016-7037(93)90429-z
- Brocas, W. M., Felis, T., Gierz, P., Lohmann, G., Werner, M., Obert, J. C., et al. (2018). Last interglacial hydroclimate seasonality reconstructed from tropical atlantic corals. *Paleoceanography and Paleoclimatology*, 33(2), 198–213. https://doi.org/10.1002/2017pa003216
- Cheng, H., Edwards, R. L., Shen, C.-C., Polyak, V. J., Asmerom, Y., Woodhead, J., et al. (2013). Improvements in ²³⁰Th dating, ²³⁰Th and ²³⁴U half-life values, and U–Th isotopic measurements by multi-collector inductively coupled plasma mass spectrometry. *Earth and Planetary Science Letters*, 371, 82–91. https://doi.org/10.1016/j.epsl.2013.04.006
- Cobb, K. M., Charles, C. D., Cheng, H., Kastner, M., & Edwards, R. L. (2003). U/Th-dating living and young fossil corals from the central tropical Pacific. Earth and Planetary Science Letters, 210(1–2), 91–103. https://doi.org/10.1016/s0012-821x(03)00138-9
- Cobb, K. M., Westphal, N., Sayani, H. R., Watson, J. T., Di Lorenzo, E., Cheng, H., et al. (2013). Highly variable El Niño–Southern Oscillation throughout the Holocene. Science, 339(6115), 67–70. https://doi.org/10.1126/science.1228246
- Cohen, A. L., & McConnaughey, T. A. (2003). Geochemical perspectives on coral mineralization. Reviews in Mineralogy and Geochemistry, 54(1), 151–187. https://doi.org/10.2113/0540151
- Corrège, T. (2006). Sea surface temperature and salinity reconstruction from coral geochemical tracers. *Palaeogeography, Palaeoclimatology*, Palaeoecology, 232(2–4), 408–428. https://doi.org/10.1016/j.palaeo.2005.10.014
- DeCarlo, T. M., D'Olivo, J. P., Foster, T., Holcomb, M., Becker, T., & McCulloch, M. T. (2017). Coral calcifying fluid aragonite saturation states derived from Raman spectroscopy. *Biogeosciences*, 14(22), 5253–5269. https://doi.org/10.5194/bg-14-5253-2017
- DeCarlo, T. M., Gaetani, G. A., Holcomb, M., & Cohen, A. L. (2015). Experimental determination of factors controlling U/Ca of aragonite precipitated from seawater: Implications for interpreting coral skeleton. *Geochimica et Cosmochimica Acta*, 162, 151–165. https://doi.org/10.1016/j.gca.2015.04.016
- Dechnik, B., Webster, J. M., Webb, G. E., Nothdurft, L., Dutton, A., Braga, J.-C., et al. (2017). The evolution of the Great Barrier reef during the last interglacial period. *Global and Planetary Change*, 149, 53–71. https://doi.org/10.1016/j.gloplacha.2016.11.018
- Delcroix, T., Alory, G., Cravatte, S., Corrège, T., & McPhaden, M. J. (2011). A gridded sea surface salinity data set for the tropical Pacific with sample applications (1950–2008). Deep Sea Research Part I: Oceanographic Research Papers, 58(1), 38–48. https://doi.org/10.1016/j.dsr. 2010.11.002

WEERABADDANA ET AL. 16 of 19

- DeLong, K. L., Quinn, T. M., Taylor, F. W., Shen, C.-C., & Lin, K. (2013). Improving coral-base paleoclimate reconstructions by replicating 350 years of coral Sr/Ca variations. *Palaeogeography*, *Palaeoclimatology*, *Palaeocology*, *373*, 6–24. https://doi.org/10.1016/j.palaeo.2012.08.019
- Doebelin, N., & Kleeberg, R. (2015). Profex: A graphical user interface for the Rietveld refinement program BGMN. *Journal of Applied Crystallography*, 48(5), 1573–1580. https://doi.org/10.1107/s1600576715014685
- Douville, E., Paterne, M., Cabioch, G., Louvat, P., Gaillardet, J., Juillet-Leclerc, A., & Ayliffe, L. (2010). Abrupt sea surface pH change at the end of the Younger Dryas in the central sub-equatorial Pacific inferred from boron isotope abundance in corals (*Porites*). *Biogeosciences*, 7(8), 2445–2459. https://doi.org/10.5194/bg-7-2445-2010
- Dutton, A., Webster, J. M., Zwartz, D., Lambeck, K., & Wohlfarth, B. (2015). Tropical tales of polar ice: Evidence of Last Interglacial polar ice sheet retreat recorded by fossil reefs of the granitic Seychelles islands. *Quaternary Science Reviews*, 107, 182–196. https://doi.org/10.1016/j. quascirev.2014.10.025
- Enmar, R., Stein, M., Bar-Matthews, M., Sass, E., Katz, A., & Lazar, B. (2000). Diagenesis in live corals from the Gulf of Aqaba. I. The effect on paleo-oceanography tracers. *Geochimica et Cosmochimica Acta*, 64(18), 3123–3132. https://doi.org/10.1016/s0016-7037(00)00417-8
- Fairbanks, R., Evans, M., Rubenstone, J., Mortlock, R., Broad, K., Moore, M., & Charles, C. (1997). Evaluating climate indices and their geochemical proxies measured in corals. Coral Reefs, 16(5), S93–S100. https://doi.org/10.1007/s003380050245
- Farfan, G. A., Apprill, A., Cohen, A., DeCarlo, T. M., Post, J. E., Waller, R. G., & Hansel, C. M. (2021). Crystallographic and chemical signatures in coral skeletal aragonite. Coral Reefs, 41(1), 19–34. https://doi.org/10.1007/s00338-021-02198-4
- Farfan, G. A., Cordes, E. E., Waller, R. G., DeCarlo, T. M., & Hansel, C. M. (2018). Mineralogy of deep-sea coral aragonites as a function of aragonite saturation state. Frontiers in Marine Science, 5. https://doi.org/10.3389/fmars.2018.00473
- Farfan, G. A., McKeown, D. A., & Post, J. E. (2023). Mineralogical characterization of biosilicas versus geological analogs. Geobiology, 21(4), 520–533. https://doi.org/10.1111/gbi.12553
- Felis, T., Giry, C., Scholz, D., Lohmann, G., Pfeiffer, M., Patzold, J., et al. (2015). Tropical Atlantic temperature seasonality at the end of the last interglacial. *Nature Communications*, 6(1), 6159. https://doi.org/10.1038/ncomms7159
- Felis, T., McGregor, H. V., Linsley, B. K., Tudhope, A. W., Gagan, M. K., Suzuki, A., et al. (2014). Intensification of the meridional temperature gradient in the Great Barrier Reef following the Last Glacial Maximum. *Nature Communications*, 5(1), 4102. https://doi.org/10.1038/propure5102
- Felis, T., Merkel, U., Asami, R., Deschamps, P., Hathorne, E. C., Kolling, M., et al. (2012). Pronounced interannual variability in tropical South Pacific temperatures during Heinrich Stadial 1. *Nature Communications*, 3, 965. https://doi.org/10.1038/ncomms1973
- Finch, A. A., & Allison, N. (2003). Strontium in coral aragonite: 2. Sr coordination and the long-term stability of coral environmental records. Geochimica et Cosmochimica Acta, 67(23), 4519–4527. https://doi.org/10.1016/s0016-7037(03)00410-1
- Griffiths, N., Müller, W., Johnson, K. G., & Aguilera, O. A. (2013). Evaluation of the effect of diagenetic cements on element/Ca ratios in aragonitic Early Miocene (~16Ma) Caribbean corals: Implications for 'deep-time' palaeo-environmental reconstructions. *Palaeogeography*, *Palaeoclimatology*, *Palaeoecology*, 369, 185–200. https://doi.org/10.1016/j.palaeo.2012.10.018
- Gross, M. G. (1964). Variations in the O¹⁸/O¹⁶ and C¹³/C¹² ratios of diagenetically altered limestones in the Bermuda Islands. *The Journal of Geology*, 72(2), 170–194. https://doi.org/10.1086/626975
- Grothe, P. R., Cobb, K. M., Liguori, G., Di Lorenzo, E., Capotondi, A., Lu, Y., et al. (2020). Enhanced El Niño–Southern Oscillation variability in recent decades. *Geophysical Research Letters*, 47(7), e2019GL083906. https://doi.org/10.1029/2019gl083906
- Gvirtzman, G., Friedman, G. M., & Miller, D. S. (1973). Control and distribution of uranium in coral reefs during diagenesis. *Journal of Sedimentary Research*, 43, 985–997. https://doi.org/10.1306/74d728ce-2b21-11d7-8648000102c1865d
- Hathorne, E. C., Felis, T., Suzuki, A., Kawahata, H., & Cabioch, G. (2013). Lithium in the aragonite skeletons of massive *Porites* corals: A new tool to reconstruct tropical sea surface temperatures. *Paleoceanography*, 28(1), 143–152. https://doi.org/10.1029/2012pa002311
- Hathorne, E. C., Gagnon, A., Felis, T., Adkins, J., Asami, R., Boer, W., et al. (2013). Interlaboratory study for coral Sr/Ca and other element/Ca ratio measurements. *Geochemistry, Geophysics, Geosystems*, 14(9), 3730–3750. https://doi.org/10.1002/ggge.20230
- Hendy, E. J., Gagan, M. K., Lough, J. M., McCulloch, M., & deMenocal, P. B. (2007). Impact of skeletal dissolution and secondary aragonite on trace element and isotopic climate proxies in *Porites* corals. *Paleoceanography*, 22(4), PA4101. https://doi.org/10.1029/2007PA001462
- Holcomb, M., DeCarlo, T. M., Gaetani, G. A., & McCulloch, M. (2016). Factors affecting B/Ca ratios in synthetic aragonite. *Chemical Geology*, 437, 67–76. https://doi.org/10.1016/j.chemgeo.2016.05.007
- Huang, B., Thorne, P. W., Banzon, V. F., Boyer, T., Chepurin, G., Lawrimore, J. H., et al. (2017). Extended reconstructed sea surface temperature, version 5 (ERSSTv5): Upgrades, Validations, and Intercomparisons. *Journal of Climate*, 30(20), 8179–8205. https://doi.org/10.1175/jcli-d-16-0836.1
- Inoue, M., Suwa, R., Suzuki, A., Sakai, K., & Kawahata, H. (2011). Effects of seawater pH on growth and skeletal U/Ca ratios of Acropora digitifera coral polyps. Geophysical Research Letters, 38(12), L12809. https://doi.org/10.1029/2011GL047786
- Inoue, M., Suzuki, A., Nohara, M., Hibino, K., & Kawahata, H. (2007). Empirical assessment of coral Sr/Ca and Mg/Ca ratios as climate proxies using colonies grown at different temperatures. *Geophysical Research Letters*, 34(12), L12611. https://doi.org/10.1029/2007gl029628
- James, N. (1972). Scleractinian coral alteration in subaerial vadose diagenetic environment. AAPG Bulletin, 56, 630.
- James, N. P. (1974a). Diagenesis of scleractinian corals in the subaerial vadose environment. Journal of Paleontology, 48, 785-799.
- James, N. P. (1974b). Diagenesis of scleractinian corals in the subaerial vadose environment. Journal of Paleontology, 785-799.
- Knutson, D. W., Buddemeier, R. W., & Smith, S. V. (1972). Coral chronometers: Seasonal growth bands in reef corals. *Science*, 177(4045), 270–272. https://doi.org/10.1126/science.177.4045.270
- Kojima, A. C., Thompson, D. M., Hlohowskyj, S. R., Carilli, J. E., Gordon, G., Goepfert, T. J., et al. (2022). A mechanistic investigation of the coral Mn/Ca-based trade-wind proxy at Kiritimati. Geochimica et Cosmochimica Acta, 328, 58–75. https://doi.org/10.1016/j.gca.2022.04.030
- Lazareth, C. E., Soares-Pereira, C., Douville, E., Brahmi, C., Dissard, D., Le Cornec, F., et al. (2016). Intra-skeletal calcite in a live-collected Porites sp.: Impact on environmental proxies and potential formation process. Geochimica et Cosmochimica Acta, 176, 279–294. https://doi.org/10.1016/j.gca.2015.12.020
- LeGrande, A. N., & Schmidt, G. A. (2006). Global gridded data set of the oxygen isotopic composition in seawater. *Geophysical Research Letters*, 33(12). https://doi.org/10.1029/2006gl026011
- Lewis, S. E., Lough, J. M., Cantin, N. E., Matson, E. G., Kinsley, L., Bainbridge, Z. T., & Brodie, J. E. (2018). A critical evaluation of coral Ba/Ca, Mn/Ca and Y/Ca ratios as indicators of terrestrial input: New data from the Great Barrier Reef, Australia. *Geochimica et Cosmochimica Acta*, 237, 131–154. https://doi.org/10.1016/j.gca.2018.06.017
- Longman, M. W. (1980). Carbonate diagenetic textures from near surface diagenetic environments. AAPG Bulletin, 64, 461–487. https://doi.org/10.1306/2f918a63-16ce-11d7-8645000102c1865d
- Lough, J. M., & Cooper, T. F. (2011). New insights from coral growth band studies in an era of rapid environmental change. *Earth-Science Reviews*, 108(3–4), 170–184. https://doi.org/10.1016/j.earscirev.2011.07.001

WEERABADDANA ET AL. 17 of 19



- 10.1029/2023PA004730
- Macintyre, I. G., & Towe, K. M. (1976). Skeletal calcite in living scleractinian corals: Microboring fillings, not primary skeletal deposits. *Science*, 193(4254), 701–702. https://doi.org/10.1126/science.193.4254.701
- Marriott, C. S., Henderson, G. M., Belshaw, N. S., & Tudhope, A. W. (2004). Temperature dependence of δ⁷Li, δ⁴⁴Ca, and Li/Ca during growth of calcium carbonate. Earth and Planetary Science Letters, 222(2), 615–624. https://doi.org/10.1016/s0012-821x(04)00149-9
- Marshall, J. (1983). Lithology and diagenesis of the carbonate foundations of modern reefs in the southern Great Barrier-Reef. BMR Journal of Australian Geology and Geophysics, 8, 253–265.
- Mavromatis, V., Montouillout, V., Noireaux, J., Gaillardet, J., & Schott, J. (2015). Characterization of boron incorporation and speciation in calcite and aragonite from co-precipitation experiments under controlled pH, temperature and precipitation rate. *Geochimica et Cosmochimica Acta*, 150, 299–313. https://doi.org/10.1016/j.gca.2014.10.024
- McCulloch, M., Fallon, S., Wyndham, T., Hendy, E., Lough, J., & Barnes, D. (2003). Coral record of increased sediment flux to the inner Great Barrier Reef since European settlement. *Nature*, 421(6924), 727–730. https://doi.org/10.1038/nature01361
- McCulloch, M., Falter, J., Trotter, J., & Montagna, P. (2012). Coral resilience to ocean acidification and global warming through pH up-regulation. *Nature Climate Change*, 2(8), 623–627. https://doi.org/10.1038/nclimate1473
- McGregor, H. V., & Abram, N. (2008). Images of diagenetic textures in *Porites* corals from Papua New Guinea and Indonesia. *Geochemistry*, Geophysics, Geosystems, 9(10). https://doi.org/10.1029/2008gc002093
- McGregor, H. V., & Gagan, M. K. (2003). Diagenesis and geochemistry of porites corals from Papua New Guinea. Geochimica et Cosmochimica Acta, 67(12), 2147–2156. https://doi.org/10.1016/s0016-7037(02)01050-5
- Min, G. R., Edwards, R. L., Taylor, F. W., Recy, J., Gallup, C. D., & Beck, J. W. (1995). Annual cycles of UCa in coral skeletons and UCa thermometry. Geochimica et Cosmochimica Acta, 59(10), 2025–2042. https://doi.org/10.1016/0016-7037(95)00124-7
- Montaggioni, L. F., Le Cornec, F., Corrège, T., & Cabioch, G. (2006). Coral barium/calcium record of mid-Holocene upwelling activity in New Caledonia, South-West Pacific. *Palaeogeography, Palaeoclimatology, Palaeoecology, 237*(2–4), 436–455. https://doi.org/10.1016/j.palaeo. 2005.12.018
- Montagna, P., McCulloch, M., Mazzoli, C., Silenzi, S., & Odorico, R. (2007). The non-tropical coral *Cladocora caespitosa* as the new climate archive for the Mediterranean: High-resolution (~weekly) trace element systematics. *Quaternary Science Reviews*, 26(3–4), 441–462. https://doi.org/10.1016/j.guascirey.2006.09.008
- Müller, A., Gagan, M. K., & McCulloch, M. T. (2001). Early marine diagenesis in corals and geochemical consequences for paleoceanographic reconstructions. *Geophysical Research Letters*, 28(23), 4471–4474. https://doi.org/10.1029/2001gl013577
- Nothdurft, L. D., & Webb, G. E. (2008). Earliest diagenesis in scleractinian coral skeletons: Implications for palaeoclimate-sensitive geochemical archives. Facies, 55(2), 161–201. https://doi.org/10.1007/s10347-008-0167-z
- Nothdurft, L. D., & Webb, G. E. (2009). Earliest diagenesis in scleractinian coral skeletons: Implications for palaeoclimate-sensitive geochemical archives. Facies. 55(2), 161–201. https://doi.org/10.1007/s10347-008-0167-z
- Nothdurft, L. D., Webb, G. E., Bostrom, T., & Rintoul, L. (2007). Calcite-filled borings in the most recently deposited skeleton in live-collected *Porites* (Scleractinia): Implications for trace element archives. *Geochimica et Cosmochimica Acta*, 71(22), 5423–5438. https://doi.org/10.1016/j.gca.2007.09.025
- Okai, T., Suzuki, A., Kawahata, H., Terashima, S. N. I., & Imai, N. (2002). Preparation of a new geological survey of Japan geochemical reference material: Coral JCp-1. Geostandards Newsletter, 26(1), 95–99. https://doi.org/10.1111/j.1751-908x.2002.tb00627.x
- O'Neil, J. R., Clayton, R. N., & Mayeda, T. K. (1969). Oxygen isotope fractionation in divalent metal carbonates. *The Journal of Chemical Physics*, 51(12), 5547–5558, https://doi.org/10.1063/1.1671982
- Pingitore, N. (1976). Vadose and phreatic diagenesis; processes, products and their recognition in corals. *Journal of Sedimentary Research*, 46, 985–1006. https://doi.org/10.1306/212f70b8-2b24-11d7-8648000102c1865d
- Quinn, T. M., & Taylor, F. W. (2006). SST artifacts in coral proxy records produced by early marine diagenesis in a modern coral from Rabaul, Papua New Guinea. *Geophysical Research Letters*, 33(4). https://doi.org/10.1029/2005g1024972
- Rabier, C., Anguy, Y., Cabioch, G., & Genthon, P. (2008). Characterization of various stages of calcitization in *Porites sp.* corals from uplifted reefs Case studies from New Caledonia, Vanuatu, and Futuna (South-West Pacific). *Sedimentary Geology*, 211(3–4), 73–86. https://doi.org/10.1016/j.sedgeo.2008.08.005
- Rahaman, W., Tarique, M., Fousiya, A. A., Prabhat, P., & Achyuthan, H. (2022). Tracing impact of El Niño Southern Oscillation on coastal hydrology using coral (87)Sr/(86)Sr record from Lakshadweep, South-Eastern Arabian Sea. *Science of the Total Environment*, 843, 157035. https://doi.org/10.1016/j.scitotenv.2022.157035
- Rahman, M. A., Halfar, J., & Shinjo, R. (2013). X-ray diffraction is a promising tool to characterize coral skeletons.
- Rashid, R., Eisenhauer, A., Liebetrau, V., Fietzke, J., Böhm, F., Wall, M., et al. (2020). Early diagenetic imprint on temperature proxies in holocene corals: A case study from French Polynesia. Frontiers in Earth Science, 8. https://doi.org/10.3389/feart.2020.00301
- Rayner, N. A., Parker, D. E., Horton, E. B., Folland, C. K., Alexander, L. V., Rowell, D. P., et al. (2003). Global analyses of sea surface temperature, sea ice, and night marine air temperature since the late nineteenth century. *Journal of Geophysical Research*, 108(D14). https://doi.org/10.1029/2002jd002670
- Reed, E. V., Thompson, D. M., & Anchukaitis, K. J. (2022). Coral-based sea surface salinity reconstructions and the role of observational uncertainties in inferred variability and trends. *Paleoceanography and Paleoclimatology*, 37(6). https://doi.org/10.1029/2021pa004371
- Reed, E. V., Thompson, D. M., Cole, J. E., Lough, J. M., Cantin, N. E., Cheung, A. H., et al. (2021). Impacts of coral growth on geochemistry: Lessons from the Galápagos Islands. *Paleoceanography and Paleoclimatology*, 36(4), e2020PA004051. https://doi.org/10.1029/2020pa004051
- Reynaud, S., Ferrier-Pagès, C., Meibom, A., Mostefaoui, S., Mortlock, R., Fairbanks, R., & Allemand, D. (2007). Light and temperature effects on Sr/Ca and Mg/Ca ratios in the scleractinian coral *Acropora sp. Geochimica et Cosmochimica Acta. Geochimica et Cosmochimica Acta*, 71(2), 354–362. https://doi.org/10.1016/j.gca.2006.09.009
- Sayani, H. R., Cobb, K. M., Cohen, A. L., Elliott, W. C., Nurhati, I. S., Dunbar, R. B., et al. (2011). Effects of diagenesis on paleoclimate reconstructions from modern and young fossil corals. Geochimica et Cosmochimica Acta, 75(21), 6361–6373. https://doi.org/10.1016/j.gca.2011.08.026
- Sayani, H. R., Thompson, D. M., Carilli, J. E., Marchitto, T. M., Chapman, A. U., & Cobb, K. M. (2021). Reproducibility of coral Mn/Ca-based wind reconstructions at Kiritimati Island and Butaritari Atoll. Geochemistry, Geophysics, Geosystems, 22(3). https://doi.org/10.1029/2020gc009398
- Schrag, D. P. (1999). Rapid analysis of high precision Sr/Ca ratios in corals and other marine carbonates. *Palaeogeography*, 14(2), 97–102. https://doi.org/10.1029/1998pa900025
- Shen, G. T., Linn, L. J., Campbell, T. M., Cole, J. E., & Fairbanks, R. G. (1992). A chemical indicator of trade wind reversal in corals from the western tropical Pacific. *Journal of Geophysical Research*, 97(C8), 12689–12697. https://doi.org/10.1029/92jc00951

WEERABADDANA ET AL. 18 of 19



- 10.1029/2023PA004730
- Sinclair, D. J. (2005). Correlated trace element "vital effects" in tropical corals: A new geochemical tool for probing biomineralization. *Geochimica et Cosmochimica Acta*, 69(13), 3265–3284. https://doi.org/10.1016/j.gca.2005.02.030
- Sinclair, D. J., Kinsley, L. P., & McCulloch, M. T. (1998). High resolution analysis of trace elements in corals by laser ablation ICP-MS. Geochimica et Cosmochimica Acta, 62(11), 1889–1901. https://doi.org/10.1016/s0016-7037(98)00112-4
- Smodej, J., Reuning, L., Wollenberg, U., Zinke, J., Pfeiffer, M., & Kukla, P. A. (2015). Two-dimensional X-ray diffraction as a tool for the rapid, nondestructive detection of low calcite quantities in aragonitic corals. *Geochemistry, Geophysics, Geosystems*, 16(10), 3778–3788. https://doi.org/10.1002/2015gc006009
- Tambutté, S., Holcomb, M., Ferrier-Pagès, C., Reynaud, S., Tambutté, É., Zoccola, D., & Allemand, D. (2011). Coral biomineralization: From the gene to the environment. *Journal of Experimental Marine Biology and Ecology*, 408(1–2), 58–78. https://doi.org/10.1016/j.jembe.2011.07.026
- Thompson, D. M. (2021). Environmental records from coral skeletons: A decade of novel insights and innovation. WIREs Climate Change, 13(1). https://doi.org/10.1002/wcc.745
- Thompson, D. M., Ault, T. R., Evans, M. N., Cole, J. E., & Emile-Geay, J. (2011). Comparison of observed and simulated tropical climate trends using a forward model of coral δ¹⁸O. *Geophysical Research Letters*, 38(14), L14706. https://doi.org/10.1029/2011GL048224
- Thompson, D. M., Cole, J. E., Shen, G. T., Tudhope, A. W., & Meehl, G. A. (2015). Early twentieth-century warming linked to tropical Pacific wind strength. *Nature Geoscience*, 8(2), 117–121. https://doi.org/10.1038/ngeo2321
- Thompson, D. M., Conroy, J. L., Konecky, B. L., Stevenson, S., DeLong, K. L., McKay, N., et al. (2022). Identifying hydro-sensitive coral δ¹⁸O records for improved high-resolution temperature and salinity reconstructions. *Geophysical Research Letters*, 49(9). https://doi.org/10.1029/2021g1096153
- Toby, B. H., & Von Dreele, R. B. (2013). GSAS-II: The genesis of a modern open-source all purpose crystallography software package. *Journal of Applied Crystallography*, 46(2), 544–549. https://doi.org/10.1107/s0021889813003531
- Tudhope, A. W., Chilcott, C. P., McCulloch, M. T., Cook, E. R., Chappell, J., Ellam, R. M., et al. (2001). Variability in the El Niño-Southern Oscillation through a glacial-interglacial cycle. *Science*, 291(5508), 1511–1517. https://doi.org/10.1126/science.1057969
- Veizer, J. (1983). Chemical diagenesis of carbonates: Theory and application of trace element technique.
- Vyverberg, K. L., Jaeger, J. M., & Dutton, A. (2018). Quantifying detection limits and uncertainty in x-ray diffraction mineralogical assessments of biogenic carbonates. *Journal of Sedimentary Research*, 88(11), 1261–1275. https://doi.org/10.2110/jsr.2018.63
- Watanabe, T. K., Watanabe, T., Pfeiffer, M., Hu, H. M., Shen, C. C., & Yamazaki, A. (2021). Corals reveal an unprecedented decrease of Arabian Sea upwelling during the current warming era. *Geophysical Research Letters*, 48(10). https://doi.org/10.1029/2021gl092432
- Weerabaddana, M., Thompson, D. M., Reed, E. V., Farfan, G., Kirk, J., Kojima, A., et al. (2023). NOAA/WDS Paleoclimatology Majuro Atoll, Marshall Islands Coral Geochemistry Data from 1947–1995 CE [Dataset]. NOAA National Centers for Environmental Information. https://doi.org/10.25921/5n8k-1161
- Weerabaddana, M. M., DeLong, K. L., Wagner, A. J., Loke, D. W. Y., Kilbourne, K. H., Slowey, N., et al. (2021). Insights from barium variability in a *Siderastrea siderea* coral in the northwestern Gulf of Mexico. *Marine Pollution Bulletin*, 173, 112930. https://doi.org/10.1016/j.marpolbul. 2021.112930
- Wei, G., Sun, M., Li, X., & Nie, B. (2000). Mg/Ca, Sr/Ca and U/Ca ratios of a *Porites* coral from Sanya Bay, Hainan Island, South China Sea and their relationships to sea surface temperature. *Palaeogeography, Palaeoclimatology, Palaeoecology, 162*(1–2), 59–74. https://doi.org/10.1016/s0031-0182(00)00105-x
- Wu, Y., Fallon, S. J., Cantin, N. E., & Lough, J. M. (2021). Assessing multiproxy approaches (Sr/Ca, U/Ca, Li/Mg, and B/Mg) to reconstruct sea surface temperature from coral skeletons throughout the Great Barrier Reef. Science of the Total Environment, 786, 147393. https://doi.org/10. 1016/i.scitotenv.2021.147393
- Zeebe, R. E. (2005). Stable boron isotope fractionation between dissolved B(OH)₃ and B(OH)₄. *Geochimica et Cosmochimica Acta*, 69(11), 2753–2766. https://doi.org/10.1016/j.gca.2004.12.011

WEERABADDANA ET AL. 19 of 19